AD_____

Award Number: W81XWH-05-1-0454

TITLE: Pepducin Based Intervention of Breast Cancer Invasion

PRINCIPLE INVESTIGATOR: Lidija Covic
Nga Nguyen
Athan Kuliopulos
Roger A. Graham

CONTRACTING ORGANIZATION: New England Medical Center
Boston, MA 02111

REPORT DATE: August 2006

TYPE OF REPORT: Final

PREPARED FOR: U.S. Army Medical Research and Materiel Command
Fort Detrick, Maryland 21702-5012

REPORT DOCUMENTATION PAGE

Form Approved
OMB No. 0704-0188

1. REPORT DATE	2. REPORT TYPE	3. DATES COVERED
01-08-2006	Final	15 Jul 2005 – 14 Jul 2006

4. TITLE AND SUBTITLE

Pepducin Based Intervention of Breast Cancer Invasion

5a. CONTRACT NUMBER

5b. GRANT NUMBER
W81XWH-05-1-0454

5c. PROGRAM ELEMENT NUMBER

6. AUTHOR(S)
Lidija Covic
Nga Nguyen
Athan Kuliopulos
Roger A. Graham

5d. PROJECT NUMBER

5e. TASK NUMBER

5f. WORK UNIT NUMBER

7. PERFORMING ORGANIZATION NAME(S) AND ADDRESS(ES)

New England Medical Center
Boston, MA 02111

8. PERFORMING ORGANIZATION REPORT NUMBER

9. SPONSORING / MONITORING AGENCY NAME(S) AND ADDRESS(ES)
U.S. Army Medical Research and Materiel Command
Fort Detrick, Maryland 21702-5012

10. SPONSOR/MONITOR'S ACRONYM(S)

11. SPONSOR/MONITOR'S REPORT NUMBER(S)

12. DISTRIBUTION / AVAILABILITY STATEMENT
Approved for Public Release; Distribution Unlimited

13. SUPPLEMENTARY NOTES
Original contains colored plates: ALL DTIC reproductions will be in black and white.

14. ABSTRACT

Matrix metalloproteases (MMPs) play a central role in remodeling the tumor-stromal microenvironment. We recently determined that stromal-derived MMP-1 also acts as a signaling molecule by cleaving protease-activated receptor 1 (PAR1) to cause breast cancer cell migration and invasion. Here, we show that ectopic PAR1 expression induces expression of the angiogenic factor Cyr61(CCN1) in breast cancer cells. The tumor-derived Cyr61 acts as an invasogenic signaling molecule that induces MMP-1 expression in adjacent stromal fibroblasts. Gene silencing of Cyr61 in breast cancer cells suppresses MMP-1 induction in stromal fibroblasts resulting in a major loss inmigration of the cancer cells towards the fibroblasts. Cyr61-dependent loss of migration was complemented byexogenous MMP-1 and required the presence of the functional PAR1 receptor on the breast cancer cells. These results suggest that interrupting tumor-stromal cell communication by targeting Cyr61 may provide an alternative therapeutic approach for the treatment of invasive breast cancer.

15. SUBJECT TERMS
Breast Cancer

16. SECURITY CLASSIFICATION OF:				18. NUMBER OF PAGES	19a. NAME OF RESPONSIBLE PERSON
a. REPORT	b. ABSTRACT	c. THIS PAGE			USAMRMC
U	U	U	UU	50	19b. TELEPHONE NUMBER *(include area code)*

Table of Contents

Paper 1: Nguyen, N., Kuliopulos, A., Graham, R. & Covic, L., (2006) Cancer Research66, 2658-65. Tumor-derived Cyr61 promotes matrix metalloprotease-1 production and PAR1-dependentmigration of breast cancer cells.

Paper 2:Boire, A., Covic, L., Agarwal, A., Jacquies S., Sherifi, S. & Kuliopulos, A. (2005) Cell 120, 303-313.PAR1 is a Matrix Metalloprotease-1 Receptor that Promotes Invasion of Breast Cancer Cells

INTRODUCTION

Matrix metalloproteases (MMPs) are a large family of zinc-dependent enzymes that cleave extracellular matrix proteins during tissue remodeling processes such as wound healing, angiogenesis and tumor invasion. Among MMPs, the collagenase MMP-1 has been identified as one of the most highly upregulated proteins in various cancers including breast, esophageal and colorectal carcinomas (1,2,3). Histological studies of tumors derived from cancer patients revealed that the majority of the MMPs, including MMP-1 are produced by stromal cells rather than tumor cells (4). Stromal MMP-1 has recently been shown to cleave and activate a G-protein-coupled receptor—the protease-activated receptor 1 (PAR-1), resulting in enhanced invasion and tumorigenesis of breast cancer cells (5,6). Thus, MMP-1 mediates tumor-stromal interactions and uncovering mechanisms that regulate MMP-1 expression may aid in blocking tumor invasion.

PAR1, an effector of MMP-1, has been identified as an oncogene (7,8,9) and is be involved in the invasive and metastatic processes of breast cancer (10), pancreatic cancer (11) and melanoma (12-17). Early studies by Bar-Shavit (10) demonstrated that PAR1 expression levels were directly correlated with degree of invasiveness in both primary breast tissue specimens and established cancer cell lines. High levels of PAR1 mRNA were found in infiltrating ductal carcinomas and very low amounts in normal and premalignant atypical intraductal hyperplasia. PAR1 expression levels increased by up to 10-fold in 106 invasive ductal and 17 invasive lobular tumors as compared to 6 normal breast specimens (18). Recent studies by our group (19) showed that the invasive MDA-MB-231 breast cancer cell line expresses very high levels of functional PAR1 whereas minimally-invasive MCF-7 cells have no PAR1. Forced expression of PAR1 in MCF7 cells was sufficient to promote tumor growth and invasion in breast cancer xenografts (5). In the present study, we set out to identify whether tumor-derived Cyr61 could induce stromal MMP-1 production and mediate tumor cell migration and invasion through PAR1

Cyr61, a member of the CCN family, is highly up-regulated during wound healing, and induces the expression of a diverse array of genes that includes MMP-1, MMP-3, TIMP1, uPA, and PAI-1, and angiogenesis and lymphogenesis factors such as VEGF-A, VEGF-C and interleukin-1β (20). Recent work suggests that the CCN family members may also play roles in contexts other than tissue repair such as tumor growth, invasion and metastasis. Interestingly, the human *Cyr61* gene was mapped to the chromosome 1p region in which abnormal rearrangements have been previously shown to correlate with poor prognosis in breast cancer patients (21,22). Upregulated expression of Cyr61 has been detected in invasive and metastatic breast cancer cells and in tumor biopsies (23). Ectopic expression of Cyr61 in MCF-7 breast cancer cells supports tumor formation and neovascularization in mice (24-27). Similar to breast tumors, Cyr61 expression in U343 glioma cells increases tumorigenicity and vascularization (28). In addition to its role in vascularization, Cyr61 can enhance motility of fibroblasts and microvascular endothelial cells (24,26), however, the mechanism of action of Cyr61 in tumor cell migration and invasion is not well understood.

In this study, we show that tumor-derived Cyr61 enhances PAR1-mediated migration of breast cancer cells towards stromal fibroblasts. We found that silencing *Cyr61* in invasive breast cancer cells caused a major loss of *MMP-1* induction from stromal fibroblasts. Conversely, silencing MMP-1 in stromal fibroblasts inhibited PAR1 and Cyr61-dependent migration. These results provide direct evidence for Cyr61 in paracrine regulation of fibroblast MMP-1 by tumor cells.

MATERIALS AND METHODS

Cell Culture and Materials. The WI38 cell line was obtained from American Type Culture Collection, and breast cancer cell lines MCF-7 and MDA-MB-231 were from the National Cancer Institute (Developmental Therapeutics, NCI/NIH, Frederick, MD). In all experiments involving MCF7 and the PAR1-MCF7 stable clones, MCF7 cells were cultured in phenol-red free RPMI-1640 media containing charcoal-stripped 10% fetal bovine serum (FBS) (Gemini Bio-Products, Calabasas, CA), 0.15% sodium bicarbonate, 10 units/ml penicillin-G, and 10 mg/ml streptomycin (Gemini Bio-Products). Conversely, with the estrogen-independent cell line MDA-MB-231, cells were cultured in phenol-red RPMI-1640 containing 10% FBS. Likewise, all fibroblast cell lines were cultured in phenol-red RPMI-1640 containing 10% FBS. During the co-culturing experiments, all cells (MCF7, MDA-MB-231, fibroblasts) were maintained in phenol-red free RPMI-1640 media plus 0.1% albumin. The Cyr61-Ab rabbit polyclonal antibody, directed against the human Cyr61 variable linker region residues G_{177}LLGKELGFDAS_{188}C, was conjugated to keyhole limpet hemacyanin (KLH) via the C-terminal cysteine. Cyr61-Ab was purified from rabbit sera by affinity chromatography using the immunizing peptide coupled to thiol-reactive beads (29).

Immunofluorescence Microscopy. Cells cultured on cover slips were washed twice with PBS, fixed with 2% formaldehyde for 20 min, washed twice with TBS and blocked with 2% BSA for 30 min at room temperature. Cells were then incubated with the Cyr61 polyclonal antibody and a MMP-9 monoclonal antibody (Oncogene Research products, Boston, MA) for 30 min at room temperature. Cells were washed five times with TBS, followed by incubation with 1:100 FITC-goat-anti-rabbit (Zymed, San Francisco, CA) and 1:100 Rhodamine-mouse secondary antibodies for 30 min at room temperature, then washed three times with TBS and mounted onto the microscope slide using 90% glycerol/10% PBS. Digital images of immunofluorescent cells were collected using a Q-Imaging Retiga 1300 digital camera and an Axioscope microscope (Carl Zeiss,

Inc., Thornwood, NY) using Open-lab digital video processing software at 40x magnification, at a resolution of 1.4 Megapixels. Images were collected using sequential excitation filters at 488 and 568 nm, and emission filters sets at 505 to 550 nm for FITC detection (green) and 585 nm for Rhodamine (red).

DNA Constructs. Protease activated receptor-1 (PAR1) was expressed from pcDEF3 (29). MCF-7 cells were transfected with pcDEF3-PAR1 and selected for resistance to neomycin using 550 μg/ml G418. The PAR1-expressing MCF-7 clone MCF7-N55 was isolated using magnetic Dynabeads M-450 that were covalently coupled to the PAR1 specific antibody, SFLLR-Ab (29). Small interfering (si)-RNA directed against Cyr61 (5-'AATGAATTGATTGCAGTTGGA-3') and firefly luciferase (5'-CGTACGCGGAATACTTCGA-3', Luci-siRNA) were synthesized by Dharmacon (Lafayette, CO). MDA-MB-231 and MCF7-N55 cells were transfected with OligofectAMINE using 20 μg siRNA per 100 mm plate (800,000 cells/plate).

Breast Cancer/Fibroblast Co-culture for Quantitative PCR. Fibroblasts (early passage 2-9) were plated on the top chamber of a transwell plate (Costar, 12 mm diameter filter, 0.4 μm pore size) at a density of 50,000/well and cultured in complete media, and starved in serum-free media (RPMI-1640 with 0.1% bovine serum albumin) one day before start of assay. Breast cancer cells were then seeded in the lower well of a transwell system and co-cultured in serum-free media for 5-40 h. For some experiments breast cancer cells were pre-treated with siRNA for Cyr61, PAR1 or luciferase (luci) control for 48 h. Fibroblasts were harvested with PBS/ 1.5 mM EDTA for RNA extraction.

Isolation of Total RNA and Quantitative PCR. Total RNA was extracted using the RNeasy mini kit (Qiagen, Valencia, CA). For semi-quantitative PCR, one microgram of RNA was reverse transcribed using Maloney murine leukemia virus (MMLV) reverse transcriptase in the presence of dNTP (0.4 μM each). cDNA was amplified in a final volume of 25 μl supplemented with 1.5 mM $MgCl_2$, dNTPs (0.2 μM

each) using Taq Polymerase (Roche Applied Science) and the following primers: hMMP-1 sense 5'-CGACTCTAGAAACACAAGAGCAAGA-3', antisense 5'-AAGGTT AGCTTACTGTCACACGCTT-3', mMMP-1 (Mcol-A) sense 5'-TCTTTATGGTCC AGGCGATGAA-3', antisense 5'-CCTCTTCTATGAGGCGGGGATA-3', actin sense 5'-GGCTCTTCCAGCCTTCCTTCCT-3', antisense 5'-CACAGAGTACTTGCGCTCA GGAGG-3'. Real-time PCR was conducted in 50 µl volumes containing 1 µl of cDNA, 25 µl of SYBR Green, 2.5 µl of 5 µM of each of the specific primers and the probe, and 19 µl of RNA-free water. All of the reactions were performed in triplicate in an iCycle iQ system (Bio-Rad, Hercules, CA, Sequence Detection System, SDS 1.9.1 alias program was used to detecting the fluorescent level of MMP1 and actin for 40 cycles, and the thermal cycling conditions of the Qiagen system were as follows: 15 min at 95˚C, 30 s at 94˚C, an h at 55 ˚C, 30 s at 72 ˚C, 15 s at 95 ˚C, 20 s at 55 ˚C, and 15 s at 95 ˚C.

Specificity of human and mouse *MMP-1* and *Cyr61* primers. Total RNA was isolated from CRL-2076 (human) and NIH-3T3 (mouse) and reverse transcribed as described in the methods section. Reverse transcribed mRNA was PCR amplified using MMP-1 specific primers or actin and visualized by ethidium bromide agarose gel electrophoresis (Supplemental Fig. 1).

Isolation of Primary Human and Mouse Mammary Fibroblasts. Mammary fat pads were removed from 3-6 week old female wild type CF-1 mice. Tissue was finely minced with a razor blade as previously described (30). Minced tissue was digested with 10 U/ml collagenase type 1 in RPMI-1640 for 20 min at 37 ˚C. The suspension was centrifuged for 10 min at 200 x g, and resuspended in 5 ml of RPMI-1640 plus 20% FBS. The resultant culture was confirmed to be fibroblastic by a pathologist. Following approval by the Tufts-NEMC Institutional Review Board, human mammary tissue was obtained from an unidentified female patient who underwent bilateral

mastectomy at Tufts-NEMC for removal of an invasive breast adenocarcinoma. Stromal fibroblasts were isolated from human breast tissue as described above.

Western Analysis. Cells were grown in 100 mm plates and cells were disrupted by multiple passage through a 27 G needle in RIPA buffer (150 mM NaCl, 50 mM Tris, pH 8.0, 0.1% SDS, 1% Nonidet P-40, 0.5% deoxycholate, 1 mM PMSF) and then incubated with heparin beads (Heparin Sepharose 6 Fast Flow, Amersham Pharmacia) at a ratio of 1:20 (slury:beads) at 4 ˚C for 1 h. The beads were washed twice with RIPA buffer containing 400 mM NaCl and eluted with 800 mM NaCl. The eluted lysate was loaded onto 12% polyacrylamide gels, and transferred to PVDF membranes (Immobilion-P, Millipore, Bedford, MA). Soluble Cyr61 from conditioned media was concentrated 10-fold with Centricon-10 (Millipore, Bedford, MA).The membrane was incubated with the Cyr61 antibody (0.16 μg/ml) at 4 ˚C for 1 h. After washing with TBS-T, the membrane was then incubated with anti-rabbit Ig-HRP antibody (Dako A/S Glostrup, Denmark) (1:1000 dilution) for 1 h at room temperature. Membrane proteins were detected by chemiluminescence (ECL, Amersham) and exposed on hyperfilm (Amersham).

Tumor-Stromal Cell Co-culturing Migration Assays. Transwell plates (24-well) (Costar, Corning, NY) with cell culture inserts 6.5 mm diameter and 8.0 μm pore size were used. Fibroblasts were seeded in the lower wells (100,000 per well) of the transwell apparatus, 2 days prior to the experiment, and starved one day before in serum-free media (RPMI-1640 with 0.1% BSA). Prior to the experiment, breast tumor cells were resuspended in serum-free media were then plated in the upper well (cell culture inserts) at a density of 50,000 (200 μL/well) and allowed to migrate to the underside of the top chamber for 40 h. The migratory cells attached to the bottom surface of the membrane were stained with Hema 3 Fixative Solution, Hema 3 Solution I, and Hema 3 Solution II (Fisher) for 30 s at room temperature. Migratory cells in 9 randomly selected migratory

fields were counted using bright-field microscopy (19). Breast cancer cells or fibroblasts were treated with siRNA and then co-cultured. For some experiments, co-culture migration assays were also performed in the presence of small molecule ligand-based antagonist of PAR1, RWJ-56110 (31,32) or APMA-activated MMP-1 (5) which was added to the lower chamber at the start of assay.

MMP-1 expression and Collagenase assay. Collagenase activity was assayed in conditioned media as previously described (5). Briefly, the cleavage of fluorescein conjugated 10 μg of DQ collagen (Molecular Probes) was assayed in 50 mM Tris-HCl (pH 7.6), 150 mM NaCl, 5 mM $CaCl_2$, and NaN_3 and cleavage was monitored continuously over time by a fluorescent microplate reader at 538 nM (excitation at 485 nM) at 25˚C. ProMMP-1 concentration was determined using Quantikine ELISA (R&D Systems, Minneapolis) according to manufacturers instructions.

Statistics. All migration results are present as mean ± SD. Comparisons were made with Student's *t* test. Statistical significance was defined as $P < 0.05$. For SYBR Green I-based quantitative PCR expression levels of target gene transcripts was quantified relative to internal β-actin expression level.

RESULTS AND DISCUSSION

PAR1 Mediated Expression of Cyr61 in Breast Cancer Cells.

To test the hypothesis that PAR1 modulates stromal MMP-1 expression through the angiogenic factor Cyr61 (Fig. 1A), we first determined whether PAR1 expression and activation induces Cyr61 expression in breast cancer cells. To conduct these studies, we used the PAR1-null breast carcinoma cell line, MCF-7, which is a poorly migratory and non-tumorigenic cell line (19), and expresses low basal levels of Cyr61 (26,33). MCF-7 cells were transiently transfected with PAR1 and activated with the strong PAR1 agonist, thrombin. Real-time (RT)-PCR analyses were used to quantify relative levels of Cyr61 mRNA. Because Cyr61 is an early response gene, we predicted that its expression would be rapidly up-regulated. Indeed, treatment of PAR1-expressing MCF-7 cells with 1 nM thrombin caused a 3.5-fold up-regulation of Cyr61 mRNA after 30 min with little effect on actin mRNA expression (Fig. 1B). Since the transfection frequency was 38%, the 3.5-fold up-regulation is probably an underestimate of PAR-1 induction. As a positive control, 17 β-estradiol (26,33) gave a 3-fold induction in Cyr61 mRNA at the 5 h time point (Fig. 1B).

Our next approach was to create a series of MCF7 cell lines that stably-expressed PAR1 and determine whether PAR1 levels correlated with basal expression of Cyr61 since PAR1 is known to stimulate oncogenic pathways (7,8) and angiogenesis (9). We generated 21 distinct clones that expressed differing levels of PAR1 on the cell surface. Clone N55 had the highest level of PAR1 expression which was similar to that of MDA-MB-231 cells (19). Clone N26 expressed intermediate levels of PAR1, whereas clone N41 had low or undetectable levels of PAR1 (Fig. 2A and C). Calcium flux measurements confirmed that PAR1 was activatable by thrombin. As shown in Fig. 2B, there was a direct correlation between PAR1 expression levels and the capacity of an individual clone to generate a thrombin-dependent Ca^{2+} signal. There was no thrombin Ca^{2+} signal in the parental MCF-7 cells.

PAR1 expression levels have been shown to directly correlate with breast cancer invasion and migration in advanced tumors. We compared different levels of PAR1 expression in the MCF7-parental background and their ability to migrate towards conditioned media from CRL-2076 fibroblasts. The N55 clone, which expressed the highest levels of PAR1, migrated ~20-fold higher frequency than the parental MCF-7 (Fig. 2C), which is comparable to the migration rate of the highly invasive MDA-MB-231 cells. Clone N26 and N29 which expressed intermediate levels of PAR1, migrated 10-fold higher than the MCF-7 cells. Clone N41 and N50, with undetectable levels of PAR1, migrated at the level of the parental MCF-7 cells.

Next, we measured the basal level of Cyr61 expression in each of the clones using western blot analysis (34) and compared Cyr61 levels to the parental MCF-7 cells and to the highly invasive MDA-MB-231 cells which are known to express high levels of Cyr61 (26). We generated a polyclonal Cyr61 antibody (Cyr61-Ab) against a peptide corresponding to the unique variable region of Cyr61 (GLLGKELGFDAS-C). Western blot analysis with the affinity-purified Cyr61-Ab detected a specific band at the expected size of 42 kDa in MDA-MB-231 cells that was absent in MCF7 cells (Fig. 2D). Interestingly, basal expression of Cyr61 directly correlated with the level of PAR1 expression with high levels of Cyr61 in clone N55, low detectable levels of Cyr61 in clones N29 and N26, and undetectable in clones N50 and 41 (Fig. 2D). However, Cyr61 protein has been reported to form high molecular aggregates (35) which may be responsible for the high molecular weight material in lanes N26 and N29. Therefore, in order to more directly determine whether PAR1-and Cyr61-expression directly correlate in PAR1-MCF7 derived clones, we measured basal mRNA expression of *Cyr61* and PAR1 (and actin) using quantitative real-time PCR analysis. We then tested whether PAR1 expression would have an effect on Cyr61 gene expression in the MCF7 clones. Surprisingly, we found a strong correlation ($R=0.99$, $p<0.005$) between *PAR1* and *Cyr61* expression (Fig. 2D). Immunohistochemical staining confirmed that clone N55 expressed high levels of Cyr61

that was secreted into the pericellular space (36) in a pattern similar to that of MDA-MB-231 (Fig. 3A-green stain). By comparison, counter-staining for tumor-derived MMP-9 (5) revealed a punctate pattern (red stain) localizing to the cell surface.

Paracrine Induction of Fibroblast MMP-1 by Breast Cancer Cells. In wound healing models, pure Cyr61 has been shown to induce secretion of MMP-1 in fibroblasts (20). Thus, we hypothesized that tumor-derived Cyr61 may have an analogous function in stimulating MMP-1 production from adjacent stromal cells which may contribute to tumor invasion (5). In order to examine a potential paracrine role of Cyr61, we developed the *in vitro* co-culturing model system shown in Fig. 3B. WI38 fibroblasts were used as stromal cells in this system because they express low basal levels of Cyr61 (Fig. 3A). We compared the high expressing-Cyr61 MDA-MB-231 and MCF7-N55 versus the low expressing-Cyr61 MCF-7 breast cancer cells (Fig. 3A) for their ability to induce *MMP-1* from the WI38 fibroblasts. The MDA-MB-231 or MCF7-N55 cells induced *MMP-1* mRNA expression in WI38 fibroblasts in the co-culturing system, whereas MCF-7 cells did not (Fig. 3C). Using quantitative RT-PCR, we showed that the presence of MDA-MB-231 cells caused a 3.5-fold induction of *MMP-1* mRNA in WI38 cells as compared to the WI38 cells grown in RPMI alone (Fig. 3C). There was no detectable change in actin mRNA levels. Furthermore, using western blot analysis we also confirmed MMP-1 induction at the protein level (Fig. 3D). We could detect the expression of both pro (~57/52 kDa) and active (42kDa) forms of MMP-1 in conditioned media from co-cultured WI38 and MDA-MB-231 cells. There was no detectable MMP-1 in WI38 cells grown alone (Fig. 3D). Previously we have shown that MDA-MB-231 cells do not express MMP-1 (5). Lastly, we used estrogen to transiently induce Cyr61 expression in the MCF-7 cells. MCF-7 cells grown in estrogen-depleted media were stimulated with 10 nM β-estradiol and co-cultured with WI38 cells. Estrogen stimulation of MCF-7 cells caused an induction of *MMP-1* from the WI38 as compared to non-stimulated MCF-7 control (Fig. 3C).

Previous studies (5) demonstrated that mRNA and protein expression levels of MMP-1 were elevated in murine tissues from MCF7-N55 xenografts (7 week old) as compared to control mammary fat pads. To mimic breast cancer cell-stromal cell interactions in vitro, we prepared fresh primary mammary fibroblasts from mouse and human tissues. Fibroblasts were used within 7 days of tissue collection without propagation. First, we confirmed that neither the MDA-MB-231 and MCF7-N55 breast cancer cells nor cells from murine mammary fat pads constitutively express *MMP-1* (5). Strikingly, there was a strong induction of *MMP-1* from the mouse and human mammary stromal fibroblasts in the presence of MCF7-N55 or MDA-MB-231 cells (Fig. 4A, B). Together, these data indicate that breast cancer cells induce expression of *MMP-1* in primary mammary stromal fibroblasts as occurred with WI38 fibroblasts. These data are consistent with previous observations which showed that MMP-1 is largely expressed by the surrounding stromal cells recruited to the invasive front of the tumor (4 ,37).

Effect of Cyr61 Gene Silencing on Paracrine Induction of Fibroblast MMP-1. In order to directly demonstrate that breast cancer cells mediate their *MMP1*-inducing effects through Cyr61, we silenced *Cyr61* gene expression using Cyr61 siRNA. As shown in Fig. 5A, treatment of MDA-MB-231 or MCF7-N55 cells with Cyr61 siRNA caused a complete loss of Cyr61 expression by western analysis and immunohistochemical staining as compared to luciferase siRNA control. Treatment of the MCF7-N55 cells with Cyr61 siRNA had little effect on expression of the closely homologous CCN family member connective tissue growth factor (CTGF) protein or PAR1 (Fig. 5B). Furthermore, treatment of the MCF7-N55 cells with PAR1 siRNA has little effect on expression of Cyr61 protein. Conversely, treatment of the MCF7-N55 cells with Cyr61 siRNA has no effect on PAR1 surface expression. The PAR1 siRNA reduces PAR1 surface expression by 80% at day 2 (these optimal conditions used here) in MDA-MB-231 cells with no effect on the expression of the closely related PAR4 gene (ref. 5, Fig. 1E). Furthermore, we

previously showed that the PAR1 siRNA treatment did not affect migration of the MDA-MB-231 cells toward IL-8.

To demonstrate that tumor cell-derived Cyr61 mediates stromal *MMP-1* induction, we co-cultured Cyr61 siRNA or luciferase siRNA-treated breast cancer cells with WI38 fibroblasts. As shown in Fig. 5C, treatment of MCF7-N55 or MDA-MB-231 cells with Cyr61 siRNA caused a 75-80% loss of *MMP-1* expression in WI38 cells as compared to control cells treated with luciferase siRNA. These data provide the first direct evidence for the involvement of cancer cell Cyr61 in paracrine regulation of fibroblast *MMP-1*.

Since MMPs are known to be regulated at the protein level, next we measured MMP-1 levels using western analysis or ELISA, and MMP-1 activity using a collagenase assay. As shown in the new Fig. 3D we found significant paracrine elevation of MMP-1 protein upon co-culturing of WI38 fibroblasts with MDA-MB-231 cells. As expected, we detected expression of predominantly the pro-form (~57/52 kDa) of MMP-1. As shown in Fig. 5D, treatment of MDA-MB-231 cells with Cyr61 siRNA results in ~40% reduction of proMMP1 as compared to PAR1- or luci-siRNA (from 3.8-4 ± 0.2 ng/ml to 2.5 ± 0.1 ng/ml) by ELISA. Conversely, co-culture with luci- or PAR1-treated MDA-MB-231 cells resulted in ~36% increase of collagenase activity. After treatment of MDA-MB-231 cells with Cyr61 siRNA, collagenase activity dropped to basal levels (WI38 cells alone). Together, these data indicate that tumor-derived Cyr61 is directly involved in regulation of stromal MMP-1.

Effect of Cyr61-MMP1 on Migration of Cancer Cells Towards Stromal Fibroblasts. We tested the ability of WI38 fibroblasts to induce PAR1-dependent chemotaxis of MDA-MB-231 cells. If the paracrine hypothesis is correct, one would predict that gene silencing of Cyr61 in co-culturing experiments would give similar effects as silencing PAR1 alone. MDA-MB-231 cells were pretreated with siRNA directed against luciferase, Cyr61 or PAR1, and placed on the top well of the Boyden chamber with WI38

fibroblasts cells in the bottom well. The ability of the MDA-MB-231 cells to migrate towards the WI38 cells was then assessed. As shown in Fig 6A, treatment of MDA-MB-231 cells with PAR1 siRNA caused a 80% loss in migration towards WI38 cells. This is consistent with our notion that PAR1 is a major mediator of migration of breast cancer cells as they migrate towards the surrounding stromal fibroblasts (5). Likewise, treatment of MDA-MB-231 cells with Cyr61 siRNA led to a similar 90% loss of migration towards the WI38 fibroblasts as compared to luciferase siRNA control (Fig. 6A).

To probe the role of MMP-1 in this tumor-stromal paracrine system, we complemented Cyr61-, PAR1- or luciferase-siRNA treated cells with activated MMP-1. Pro-MMP1 was first activated with aminophenylmercuric acetate (APMA) and then dialyzed to remove the cytotoxic mercury compound. As shown in Fig. 6A, B, Cyr61-siRNA-treated, but not PAR1-siRNA-treated MDA-MB-231 or MCF7-N55 cells, could be complemented with 1 nM MMP-1. Furthermore, the regain of migration was completely abrogated by pharmacological blockade of PAR1 with 1 μM RWJ-56110 (32). As expected, there was no MMP1-dependent enhancement in migration of PAR1-siRNA-treated MDA-MB-231 or MCF7-N55 cells. Similar results were obtained using either WI38 or human primary mammary stromal fibroblasts (Fig. 6B). These data demonstrate that the effect of MMP-1 on MDA-MB-231 or MCF7-N55 cell migration towards fibroblasts is PAR1-dependent. Likewise, we showed that co-culturing of Cyr61-positive tumor cells with fibroblasts or conditioned media rescues the defect in migration of Cyr61 siRNA-treated tumor cells (Supplemental Fig. 2). However, tumor PAR1 is essential for this migration process and is not rescued by the Cyr61-positive cells. Together, these results strongly support a paracrine role for tumor-derived Cyr61 in induction of stromal cell MMP-1 that leads to PAR1-dependent cell migration.

Lastly, in order to confirm that stromal-derived MMP-1 was indeed mediating breast cancer cell migration, we knocked down MMP-1 expression in fibroblasts, and co-cultured the fibroblasts with breast cancer cells. MCF7-N55 cells were pretreated with

siRNA directed against Cyr61, PAR1 or luciferase, and placed on the top well of the Boyden chamber with MMP1-siRNA treated fibroblasts in the bottom well. As shown in Fig. 6C, treatment of fibroblasts with MMP1-siRNA attenuated 50% of chemotaxis of MCF7-PAR1/N55 cells as compared to the luciferase-siRNA-treated fibroblasts. The level of inhibition achieved by MMP1-siRNA treatment of the fibroblasts was similar to that of Cyr61- or PAR1-siRNA-treatment of the MCF7-N55 cells. These results confirm that fibroblast-derived MMP-1 mediates migration of these MCF7/PAR1-expressing cells.

CONCLUSIONS

Cyr61 has been previously proposed to regulate cutaneous wound healing by induction of genes such as MMPs (20). Matrix remodeling by the MMPs including interstitial collagenase, MMP-1, is essential for the wound healing process. More recent studies have shown that MMP-1 is marker of poor prognosis in breast, colorectal and esophageal cancers (1,2,38). The PAR1 receptor was identified as an effector molecule for MMP-1 and was found to promote breast cancer cell migration and invasion (5). Here, we present the first evidence that breast cancer cells use Cyr61 to instruct stromal fibroblasts to produce MMP-1 which in turn stimulates PAR1-dependent cancer cell migration. Interestingly, gain-of-constitutive Cyr61 expression was achieved by stably expressing PAR1 in MCF7 cells. These Cyr61-expressing MCF7 cells form tumors that are highly invasive in nude mouse models (5). We show that gene silencing of Cyr61 results in nearly complete inhibition of migration and invasion of breast cancer cells towards stromal fibroblasts. Moreover, it has been shown that forced overexpression of Cyr61 results in a more invasive, tumorigenic MCF-7 cell line in the absence of estrogen, and many aggressive breast cancers express high levels of Cyr61 (23,26,27). Thus, gain-of-constitutive Cyr61 expression may be an important event in the progression of breast cancer towards a more invasive phenotype.

Acknowledgments

We thank Dr. Sridhar Pal for assistance with fibroblast cutures, Dr. Steve Swift for helpful discussions, and Dr. John Erban for his support. We are grateful to Claudia Derian and Patricia Andrade-Gordon of Johnson and Johnson Pharmaceuticals for providing RWJ-56110. This research was supported by NIH grants CA104406 (L.C), HL64701 (A.K.) and HL57905 (A.K.), and US Army BC045321 (L.C.).

REFERENCES

(1) Poola, I., DeWitty, R. L., Marshalleck, J. J., Bhatnagar, R., Abraham, J., and Leffall, L. D. (2005) Identification of MMP-1 as a putative breast cancer predictive marker by global gene expression analysis. *Nature Medicine 11*, 481-483.

(2) Murray, G. I., Duncan, M. E., O'Neil, P., McKay, J. A., Melvin, W. T., and Fothergill, J. E. (1998) Matrix metalloproteinase-1 is associated with poor prognosis in oesophageal cancer. *J. Pathol. 185*, 256-261.

(3) Migita, T., Sato, E., Saito, K., Mizoi, T., K., S., S.Matsuno, Nagura, H., and Ohtani, H. (1999) Differing expression of MMPs-1 and -9 and urokinase receptor between diffuse- and intestinal-type gastric carcinoma. *Int J Cancer 84*, 74-79.

(4) Heppner, K. J., Matrisian, L. M., Jensen, R. A., and Rodgers, W. H. (1996) Expression of Most Matrix Metalloprotease Family Members in Breast Cancer Represents a Tumor-Induced Host Response. *Am. J. Pathol. 149*, 273-282.

(5) Boire, A., Covic, L., Agarwal, A., Jacques, S., Sherifi, S., and Kuliopulos, A. (2005) PAR1 is a Matrix Metalloprotease-1 Receptor that Promotes Invasion and Tumorigenesis of Breast Cancer Cells. *Cell 120,* 303-313.

(6) Arribas, J. (2005) Matrix Metalloproteases and Tumor Invasion. *N Engl J Med 352*, 2020-2021.

(7) Whitehead, I., Kirk, H., and Kay, R. (1995) Expression Cloning of Oncogenes by Retroviral Transfer of cDNA Libraries. *Mol. Cell. Biol. 15*, 704-710.

(8) Martin, C. B., Mahon, G. M., Klinger, M. B., Kay, R. J., Symons, M., Der, C. J., and Whitehead, I. P. (2001) The thrombin receptor, PAR-1, causes transformation by activation of Rho-mediated signaling pathways. *Oncogene 20*, 1953-1963.

(9) Yin, Y.-J., Salah, Z., Maoz, M., Ram, S. C. E., Ochayon, S., Neufeld, G., Katzav, S., and Bar-Shavit, R. (2003) Oncogenic transformation induces tumor angiogenesis: a role for PAR1 activation. *FASEB J. 17*, 163-174.

(10) Even-Ram, S., Uziely, B., Cohen, P., Grisaru-Granovsky, S., Maoz, M., Ginzburg, Y., Reich, R., Vlodavsky, I., and Bar-Shavit, R. (1998) Thrombin Receptor Overexpression in Malignant and Physiological Invasion Processes. *Nature Med. 4*, 909-914.

(11) Rudroff, C., Seibold, S., Kaufmann, R., Zetina, C. C., Reise, K., Schafer, U., Schneider, A., Brockmann, M., Scheele, J., and Neugebauer, E. A. (2002) Expression of the thrombin receptor PAR-1 correlates with tumour cell differentiation of pancreatic adenocarcinoma in vitro. *Clin. Exp. Metastasis 19*, 181-189.

(12) Nierodzik, M. L., Chen, K., Takeshita, K., Li, J. J., Huang, Y. Q., Feng, X. S., D'Andrea, M. R., Andrade-Gordon, P., and Karpatkin, S. (1998) Protease-activated receptor 1 (PAR-1) is required and rate-limiting for thrombin-enhanced experimental pulmonary metastasis. *Blood 92*, 3694-3700.

(13) Even-Ram, S. C., Maoz, M., Pokroy, E., Reich, R., Katz, B.-Z., Gutwein, P., Altevogt, P., and Bar-Shavit, R. (2001) Tumor Cell Invasion Is Promoted by Activation of Protease Activated Receptor-1 in Cooperation with the alpha vbeta 5 Integrin. *J. Biol. Chem. 276*, 10952-10962.

(14) Nierodzik, M. L., Kajumo, F., and Karpatkin, S. (1992) Effect of thrombin treatment of tumor cells on adhesion of tumor cells to platelets in vitro and metstasis in vivo. *Cancer Res 52*, 3267-3272.

(15) Tellez, C., and Bar-Eli, M. (2003) Role and regulation of the thrombin receptor (PAR-1) in human melanoma. *Oncogene 22*, 3130-3137.

(16) Tellez, C., McCarty, M., Ruiz, M., and Bar-Eli, M. (2003) Loss of Activator Protein-2α Results in Overexpression of Protease-activated Receptor-1 and Correlates with the Malignant Phenotype of Human Melanoma. *J. Biol. Chem. 278*, 46632-42.

(17) Hazarika, P., McCarty, M. F., Prieto, V. G., George, S., Babu, D., Koul, D., Bar-Eli, M., and Duvic, M. (2004) Up-regulation of Flotillin-2 is associated with

melanoma progression and modulates expression of the thrombin receptor protease activated receptor 1. *Cancer Res. 64,* 7361-9.

(18) Korkola, J. E., DeVries, S., Fridlyand, J., Hwang, E. S., Estep, A. L. H., Chen, Y.-Y., Chew, K. L., Dairkee, S. H., Jensen, R. M., and Waldman, F. M. (2003) Differentiation of Lobular versus Ductal Breast Carcinomas by Expression Microarray Analysis. *Cancer Res. 63,* 7167-7175.

(19) Kamath, L., Meydani, A., Foss, F., and Kuliopulos, A. (2001) Signaling from Protease-activated Receptor-1 Inhibits Migration and Invasion of Breast Cancer Cells. *Cancer Res. 61,* 5933-5940.

(20) Chen, C.-C., Chen, N., and Lau, L. F. (2001) The Angiogenic Factors Cyr61 and Connective Tissue Growth Factor Induce Adhesive Signaling in Primary Human Skin Fibroblasts. *J. Biol. Chem. 276,* 10443-10452.

(21) Liotta, L. A., and Kohn, E. C. (2001) The microenvironment of the tumour-host interface. *Nature 411,* 375-379.

(22) Ito, A., Mukaiyama, A., Itoh, Y., Nagase, H., Thogersen, I. B., Enghild, J. J., Sasaguri, Y., and Mori, Y. (1996) Degradation of Interleukin 1β by Matrix Metalloproteinases. *J. Biol. Chem. 271,* 14657-14660.

(23) Tsai, M. S., Hornby, A. E., Lakins, J., and Lupu, R. (2000) Expression and function of CYR61, an angiogenic factor, in breast cancer cell lines and tumor biopsies. *Cancer Res. 60,* 5603-5607.

(24) Babic, A. M., Kireeva, M. L., Kolesnikova, T. V., and Lau, L. F. (1998) CYR61, a product of a growth factor-inducible immediate early gene, promotes angiogenesis and tumor growth. *Proc. Natl. Acad. Sci. (USA) 95,* 6355-6360.

(25) Bork, P. (1993) The modular architecture of a new family of growth regulators related to connective tissue growth factor. *FEBS Lett. 26,* 125-130.

(26) Xie, D., Miller, C. W., O'Kelly, J., Nakachi, K., Sakashita, A., Said, J. W., Gornbein, J., and Koeffler, H. P. (2001) Breast Cancer. Cyr61 Is Overexpressed,

Estrogen-Inducible, and Associated with More Advanced Disease. *J. Biol. Chem. 276*, 14187-14194.

(27) Walter-Yohrling, J., Pratt, B. M., Ledbetter, S., and Teicher, B. A. (2003) Myofibroblasts enable invasion of endothelial cells into three-dimensional tumor cell clusters: a novel in vitro tumor model. *Cancer Chemother Pharmacol. 52,* 263-269.

(28) Xie, D., Yin, D., Tong, X., O'Kelly, J., Mori, A., Miller, C., Black, K., Gui, D., Said, J. W., and Koeffler, H. P. (2004) Cyr61 is overexpressed in gliomas and involved in integrin-linked kinase-mediated Akt and beta-catenin-TCF/Lef signaling pathways. *Cancer Res 64,* 1987-96.

(29) Kuliopulos, A., Covic, L., Seeley, S. K., Sheridan, P. J., Helin, J., and Costello, C. E. (1999) Plasmin Desensitization of the PAR1 Thrombin Receptor: Kinetics, Sites of Truncation, and Implications for Thrombolytic Therapy. *Biochemistry 38,* 4572-4585.

(30) Reiter, L. A., Rizzi, J. P., Pandit, J., Lasut, M. J., McGahee, S. M., Parikh, V. D., Blake, J. F., Danley, D. E., Laird, E. R., Lopez-Anaya, A., Lopresti-Morrow, L. L., Mansour, M. N., Martinelli, G. J., Mitchell, R. G., Owens, B. S., Pauly, T. A., Reeves, L. M., Schulte, G. K., and Yocum, S. A. (1999) Inhibition of MMP-1 and MMP-13 with phosphinic acids that exploit binding in the S2 pocket. *Bioorg. Med. Chem. Lett. 9*, 127-132.

(31) Bernatowicz, M. S., Klimas, C. E., Hartl, K. S., Peluso, M., Allegretto, N. J., and Seiler, S. M. (1996) Development of Potent Thrombin Receptor Antagonist Peptides. *J. Med. Chem. 39*, 4879-4887.

(32) Andrade-Gordon, P., Maryanoff, B. E., Derian, C. K., Zhang, H.-C., Addo, M. F., Darrow, A. L., Eckardt, A. J., Hoekstra, W. J., McComsey, D. F., Oksenberg, D., Reynolds, E. E., Santulli, R. J., Scarborough, R. M., Smith, C. E., and White, K. B. (1999) Design, synthesis, and biological characterization of a peptide-mimetic antagonist for a tethered-ligand receptor. *Proc. Natl. Acad. Sci. (USA) 96,* 12257-12262.

(33) Sampath, D., Winneker, R. C., and Zhang, Z. (2001) Cyr61, a member of the CCN family, is required for MCF-7 cell proliferation: regulation by 17beta-estradiol and overexpression in human breast cancer. *Endocrinology 142*, 2540-2548.

(34) Muramatsu, Y., Tsujie, M., Kohda, Y., Pham, B., Perantoni, A. O., Zhao, H., Jo, S. K., Yuen, P. S., Craig, L., Hu, X., and Star, R. A. (2002) Early detection of cysteine rich protein 61 (CYR61, CCN1) in urine following renal ischemic reperfusion injury. *Kindney Int. 62*, 1601-1610.

(35) Kireeva, M. L., E., F., Yang, G. P., and Lau, L. F. (1996) Cyr61, a product of a growth factor-inducible immediate-early gene, promotes cell proliferation, migration, and adhesion. *Mol. Cell. Biol. 16*, 1326-1334.

(36) Yang, G. P., and Lau, L. F. (1991) Cyr61, product of a growth factor-inducible immediate early gene, is associated with the extracellular matrix and the cell surface. *Cell. Growth. Differ. 2*, 351-357.

(37) Davies, B., Miles, D. W., and Happerfield, L. C. (1993) Activity of type IV Collagenases in Benign and Malignant Breast Disease. *Br. J. Cancer 67*, 1126-1131.

(38) Veer, L. J. v. '., Dai, H., Vijver, M. J. v. d., He, Y. D., Hart, A. A., Mao, M., Peterse, H. L., Kooy, K. v. d., Marton, M. J., Witteveen, A. T., Schreiber, G. J., Kerkhoven, R. M., Roberts, C., Linsley, P. S., Bernards, R., and Friend, S. H. (2002) Gene expression profiling predicts clinical outcome of breast cancer. *Nature 415*, 530-536.

FIGURE LEGENDS

Figure 1. Activation of PAR1 induces *Cyr61* mRNA expression in breast cancer cells. **A,** a model for tumor-derived Cyr61 induction of stromal matrix metalloprotease-1 that results in enhanced tumor cell migration. **B,** MCF-7 cells transiently transfected with PAR1 were stimulated with thrombin (1 nM) for 0.5-2 h or 17 β-estradiol (E2, 100 nM) for 5 h. Transfection efficiency was 38%. Expression levels of Cyr61 (CCN1) and actin were determined using SYBR green I-based quantitative PCR. Similar conditions and total amount of RNA were used in each experiment. The relative Cyr61 gene expression was normalized to the mean value of non-stimulated MCF7 cells transiently transfected with PAR1 (non-induced control), and this value was set to 1. Each of the thrombin-induced time points was divided by the actin control conducted in the identical sample to generate the relative fold-induction for Cyr61. The experiments were repeated twice and the indicated values are the mean of triplicate points ± sd with similar results.

Figure 2. Correlation of PAR1 and Cyr61 expression in stable PAR1-MCF-7 cell lines. **A,** PAR1 expression profiles of PAR1-MCF7 clones. Individual PAR1-MCF7 clones: N41, N11, N26 and N55 were labeled with SFLLRN-Ab (1 μg/mL) and treated with FITC-labeled secondary antibody and analyzed by flow cytometry. **B,** Functional activity of PAR1 in PAR1-MCF7 cell lines. Intracellular calcium fluxes in response to 3 nM thrombin were measured on a Perkin-Elmer LS50B Spectrofluorimeter. Cells were labeled with 2.5 μM fura2/AM and Ca^{2+} fluorescence experiments were performed with emission recorded at 510 nm and dual excitation at 340 and 380 nm. **C,** Migration of PAR1-MCF7 clones and MCF7 parental cell line towards fibroblast (CRL-2076) conditioned media. Migration (50,000 cells/upper well) was measured in a Transwell apparatus as previously described (19). **D,** Correlation of quantitative real-time PCR analysis of the *PAR1* and *Cyr61* in MCF7, MDA-MB-231, N55 and N26 cells. Cyr61 and PAR1 expression levels were normalized to the reference gene β-actin to correct for variation in the amount of RNA

amplified between different cell types. Actin-normalized Cyr61 mRNA levels are plotted on the y-axis as a function of normalized PAR1 mRNA levels for MCF7, MCF7-N26, MCF7-N55 and MDA-MB-231 breast cancer cells. Western analysis of Cyr61 from extracellular matrix (ECM) of breast tumor cells. The expression levels of ECM-bound Cyr61 protein were detected with a polyclonal Cyr61-Ab as described in methods section.

Figure 3. Breast cancer cells induce expression of *MMP-1* in fibroblasts. **A,** Expression of Cyr61 protein in extracellular matrix (ECM) of breast tumor cells and fibroblasts. The expression levels of ECM-bound Cyr61 protein were detected by immunoblot analysis using polyclonal Cyr61-Ab. Cells grown on cover slips were stained with anti-human Cyr61 and MMP-9 antibodies, fluorescently labeled and photographed (x400 magnification). Antibody against MMP-9 was used to stain for localization of tumor cells. **B,** schematic representation of co-culturing assay for tumor-mediated induction of fibroblast derived *MMP-1*. **C,** Presence of MDA-MB-231 or MCF7-N55 tumor cells causes induction of *MMP-1* mRNA expression in WI38 cells. Reverse transcription and PCR of MMP-1 or actin product was generated using cDNA template isolated from WI38 co-cultured with cancer cells. The amplification of actin was carried out to verify that a comparable amount of cDNA was analyzed. Quantitative real-time PCR analysis of *MMP-1* expression in WI38 cells co-cultured in presence of MDA-MB-231 cells for 5 h. MMP-1 mRNA expression levels were normalized to the reference gene β-actin to correct for variation in the amount of RNA amplified. Actin-normalized MMP-1 mRNA levels are plotted on y-axis as a function of RT-PCR cycle number. **D,** Western blot analysis of conditioned media from WI38 cells alone or WI38/MDA-MB-231 co-culture using MMP-1 ab (AB806, Chemicon International).

Figure 4. PAR1-expressing breast cancer cells promote MMP-1 production in primary mammary fibroblasts. Primary mouse (**A**) or human (**B**) mammary fibroblasts were co-

cultured for 20 h with breast cancer cells MDA-MB-231 or MCF7-N55. MMP-1 mRNA expression levels in the three different fibroblast cells were normalized to the reference gene β-actin to correct for variation in the amount of RNA amplified between different cell types. Actin-normalized MMP-1 mRNA levels are plotted on y-axis as a function of RT-PCR cycle number.

Figure 5. Silencing of *Cyr61* in breast cancer cells down-regulates *MMP-1* expression levels in fibroblasts. **A,** Effect of Cyr61-siRNA on Cyr61 protein expression in MDA-MB-231 or MCF7-N55 cells. Protein was purified using heparin beads and western analysis performed using the Cyr61-Ab. Immunohistochemical staining using the Cyr61-Ab of Luci-siRNA or Cyr61 siRNA-treated MCF7-N55 cells. **B,** Effect of Cyr61-siRNA and PAR1-siRNA on protein expression of CTGF or Cyr61. PAR1 expression profiles of MCF7-N55 treated with Cyr61- or luci-siRNA, labeled with SFLLRN-Ab (1 μg/mL) and analyzed by flow cytometry. **C,** quantitative real-time PCR analysis of the *MMP-1* expression in WI38 cells co-cultured for 24 h in the presence of MCF7-N55 or MDA-MB-231 cells treated with Luci-siRNA or Cyr61-siRNA. The relative MMP-1 gene expression was normalized to the mean value of non-stimulated WI38 cells (non-induced control), and this value was set to 1. MMP-1 RT-PCR of each of the siRNA-treated N55 samples was divided by the actin control conducted in the identical sample to generate the relative fold-induction for MMP-1. **D,** Collagenase activity of conditioned media from WI38 and MDA-MB-231 co-cultures treated with either luci, PAR1- or Cyr61-siRNA.

Figure 6. Exogenous MMP-1 complements the Cyr61 defect in PAR1-mediated breast cancer cell migration. **A and B,** MDA-MB-231 and MCF7-N55 cells were treated for 48 h with Cyr61-siRNA, PAR1-siRNA or luciferase-siRNA and allowed to migrate towards fibroblasts grown in lower chamber (100,000/lower well) of a transwell plate in 600 μl of

RPMI-1640/0.1% BSA. APMA-activated MMP-1 (1 nM) and/or RWJ-56110 (1 μM) were added as indicated. **C,** MCF7-N55 (upper well) and NIH-3T3 cells (lower well) were treated for 48 h with siRNA (Cyr61-, PAR1-, Luci- or MMP-1) as indicated. siRNA treated MCF7-N55 cells (upper chamber) were allowed to migrated towards Luci- or MMP1-siRNA treated NIH-3T3 cells (lower chamber) in 600 μl of RPMI-1640/0.1% BSA. Total number of cells that migrated over 40 h period was counted by microscopy. Each data point represents the mean ± SD.

Supplemental Figure. 1. A-C, shows specificity of human and mouse *MMP-1* and *Cyr61* primers tested in CRL-2076 (H=human) and NIH-3T3 (M=mouse) cells. Total RNA was isolated and reverse transcribed as described in the methods section. Reverse transcribed mRNA was PCR amplified using MMP-1 specific primers or actin and visualized by ethidium bromide agarose gel electrophoresis. **D,** characterization of MCF7-N55 breast cancer cells for MMP-1 and Cyr61 expression.

Supplemental Figure. 2. Co-culturing Cyr61-positive breast cancer cells or conditioned meida plus WI38 fibroblasts rescues the defect in migration of breast cancer cells treated with Cyr61-siRNA. MDA-MB-231 and MCF7-N55 cells were treated for 48 h with Cyr61-siRNA, PAR1-siRNA or luciferase-siRNA and allowed to migrate for 40 h toward WI38 fibroblasts plus breast cancer cells grown in the lower chamber (WI38 cells (100,000) plus breast cancer cells (50,000) in lower well) of a transwell plate in 600 μl of RPMI-1640/0.1% BSA or conditioned media from breast cancer cells plus WI38 fibroblasts.

Key Research Accomplishments

The angiogenesis factor Cyr61 is overexpressed in invasive and metastatic breast cancer cells and in tumor biopsies. Recombinant Cyr61 has also been reported to be a major stimulator of matrix metalloproteases during wound healing. Nguyen et al. show that breast cancer cells and stromal fibroblasts communicate via Cyr61 to produce the matrix metalloprotease MMP-1 which in turn stimulates cancer cell migration by directly cleaving the G protein coupled receptor, PAR1. These findings suggest that blocking Cyr61 may provide a new therapeutic strategy to target tumor-stromal communication in cancer. This work was recently published in *Cancer Research* (66: 2658-65).

We also recently made highly original discovery that matrix metalloprotease-1 (MMP-1) secreted by host fibroblasts promotes tumor-cell growth and invasion by directly cleaving and activating PAR1 that was published in *Cell* (120:303-13). We have continued investigation using pepducin technology in development of therapeutics against PAR1.

Tumor-Derived Cyr61(CCN1) Promotes Stromal Matrix Metalloproteinase-1 Production and Protease-Activated Receptor 1–Dependent Migration of Breast Cancer Cells

Nga Nguyen, Athan Kuliopulos, Roger A. Graham, and Lidija Covic

Division of Hematology/Oncology, Molecular Oncology Research Institute, New England Medical Center and Departments of Medicine, Tufts University School of Medicine, Boston, Massachusetts

Abstract

Matrix metalloproteinases (MMPs) play a central role in remodeling the tumor-stromal microenvironment. We recently determined that stromal-derived MMP-1 also acts as a signaling molecule by cleaving protease-activated receptor 1 (PAR1) to cause breast cancer cell migration and invasion. Here, we show that ectopic PAR1 expression induces expression of the angiogenic factor Cyr61(CCN1) in breast cancer cells. The tumor-derived Cyr61 acts as an invasogenic signaling molecule that induces MMP-1 expression in adjacent stromal fibroblasts. Gene silencing of Cyr61 in breast cancer cells suppresses MMP-1 induction in stromal fibroblasts resulting in a major loss in migration of the cancer cells toward the fibroblasts. Cyr61-dependent loss of migration was complemented by exogenous MMP-1 and required the presence of the functional PAR1 receptor on the breast cancer cells. These results suggest that interrupting tumor-stromal cell communication by targeting Cyr61 may provide an alternative therapeutic approach for the treatment of invasive breast cancer. (Cancer Res 2006; 66(5): 2658-65)

Introduction

Matrix metalloproteinases (MMPs) are a large family of zinc-dependent enzymes that cleave extracellular matrix proteins during tissue remodeling processes, such as wound healing, angiogenesis, and tumor invasion. Among MMPs, the collagenase MMP-1 has been identified as one of the most highly up-regulated proteins in various cancers, including breast, esophageal, and colorectal carcinomas (1–3). Histologic studies of tumors derived from cancer patients revealed that the majority of the MMPs, including MMP-1, are produced by stromal cells rather than tumor cells (4). Stromal MMP-1 has recently been shown to cleave and activate a G-protein-coupled receptor, the protease-activated receptor 1 (PAR1), resulting in enhanced invasion and tumorigenesis of breast cancer cells (5, 6). Thus, MMP-1 mediates tumor-stromal interactions, and uncovering mechanisms that regulate MMP-1 expression may aid in blocking tumor invasion.

PAR1, an effector of MMP-1, has been identified as an oncogene (7–9) and is involved in the invasive and metastatic processes of breast cancer (10), pancreatic cancer (11), and melanoma (12–17). Early studies by Even-Ram et al. (10) showed that PAR1 expression levels were directly correlated with degree of invasiveness in both primary breast tissue specimens and established cancer cell lines. High levels of PAR1 mRNA were found in infiltrating ductal carcinomas and very low amounts in normal and premalignant atypical intraductal hyperplasia. *PAR1* expression levels increased by up to 10-fold in 106 invasive ductal and 17 invasive lobular tumors compared with 6 normal breast specimens (18). Recent studies by our group (19) showed that the invasive MDA-MB-231 breast cancer cell line expresses very high levels of functional PAR, whereas minimally invasive MCF7 cells have no PAR1. Forced expression of PAR1 in MCF7 cells was sufficient to promote tumor growth and invasion in breast cancer xenografts (5). In the present study, we set out to identify whether tumor-derived Cyr61 could induce stromal MMP-1 production and mediate tumor cell migration and invasion through PAR1.

Cyr61, a member of the CCN family, is highly up-regulated during wound healing and induces the expression of a diverse array of genes, such as *MMP-1, MMP-3,* tissue inhibitor of metalloproteinase 1, urokinase-type plasminogen activator, and plasminogen activator inhibitor-1, and angiogenesis and lymphogenesis factors, such as vascular endothelial growth factor (*VEGF*)*-A, VEGF-C,* and interleukin (*IL*)*-1β* (20). Recent work suggests that the CCN family members may also play roles in contexts other than tissue repair, such as tumor growth, invasion, and metastasis. Interestingly, the human *Cyr61* gene was mapped to the chromosome 1p region in which abnormal rearrangements have been shown previously to correlate with poor prognosis in breast cancer patients (21, 22). Up-regulated expression of Cyr61 has been detected in invasive and metastatic breast cancer cells and tumor biopsies (23). Ectopic expression of Cyr61 in MCF7 breast cancer cells supports tumor formation and neovascularization in mice (24–27). Similar to breast tumors, Cyr61 expression in U343 glioma cells increases tumorigenicity and vascularization (28). In addition to its role in vascularization, Cyr61 can enhance motility of fibroblasts and microvascular endothelial cells (24, 26); however, the mechanism of action of Cyr61 in tumor cell migration and invasion is not well understood.

In this study, we show that tumor-derived Cyr61 enhances PAR1-mediated migration of breast cancer cells toward stromal fibroblasts. We found that silencing *Cyr61* in invasive breast cancer cells caused a major loss of MMP-1 induction from stromal fibroblasts. Conversely, silencing MMP-1 in stromal fibroblasts inhibited PAR1- and Cyr61-dependent migration. These results provide direct evidence for Cyr61 in paracrine regulation of fibroblast MMP-1 by tumor cells.

Materials and Methods

Cell culture and materials. The WI38 cell line was obtained from American Type Culture Collection (Manassas, VA), and breast cancer cell

Note: Supplementary data for this article are available at Cancer Research Online (http://cancerres.aacrjournals.org/).

Requests for reprints: Lidija Covic, Division of Hematology/Oncology, Molecular Oncology Research Institute, New England Medical Center, Box 7510, 75 Kneeland Street, Boston, MA 02111. Fax: 617-636-7855; E-mail: lcovic@tufts-nemc.org.

doi:10.1158/0008-5472.CAN-05-2082

lines MCF7 and MDA-MB-231 were from the Developmental Therapeutics, National Cancer Institute/NIH (Frederick, MD). In all experiments involving MCF7 and the PAR1-MCF7 stable clones, MCF7 cells were cultured in phenol red–free RPMI 1640 containing charcoal-stripped 10% fetal bovine serum (FBS; Gemini Bio-Products, Calabasas, CA), 0.15% sodium bicarbonate, 10 units/mL penicillin G, and 10 mg/mL streptomycin (Gemini Bio-Products). Conversely, with the estrogen-independent cell line MDA-MB-231, cells were cultured in phenol red–free RPMI 1640 containing 10% FBS. Likewise, all fibroblast cell lines were cultured in phenol red–free RPMI 1640 containing 10% FBS. During the coculturing experiments, all cells (MCF7, MDA-MB-231, fibroblasts) were maintained in phenol red–free RPMI 1640 plus 0.1% albumin. The Cyr61 antibody rabbit polyclonal antibody, directed against the human Cyr61 variable linker region, residues G_{177}LLGKELGFDAS$_{188}$C, was conjugated to keyhole limpet hemocyanin via the COOH-terminal cysteine. Cyr61 antibody was purified from rabbit sera by affinity chromatography using the immunizing peptide coupled to thiol-reactive beads (29).

Immunofluorescence microscopy. Cells cultured on coverslips were washed twice with PBS, fixed with 2% formaldehyde for 20 minutes, washed twice with TBS, and blocked with 2% bovine serum albumin (BSA) for 30 minutes at room temperature. Cells were then incubated with the Cyr61 polyclonal antibody and a MMP-9 monoclonal antibody (Oncogene Research Products, Boston, MA) followed by incubation with 1:100 FITC goat anti-rabbit (Zymed, San Francisco, CA) and 1:100 rhodamine mouse secondary antibodies. Digital images of immunofluorescent cells were collected using a Q-Imaging Retiga 1300 digital camera and an Axioscope microscope (Carl Zeiss, Inc., Thornwood, NY) using Open-lab digital video processing software at ×40 magnification and a resolution of 1.4 MP. Images were collected using sequential excitation filters at 488 and 568 nm and emission filters at 505 to 550 nm for FITC detection (green) and 585 nm for rhodamine (red).

DNA constructs. PAR1 was expressed from pcDEF3 (29). MCF7 cells were transfected with pcDEF3-PAR1, and individual clones were selected as described previously (5). Small interfering RNAs (siRNA), directed against Cyr61 (5′-AATGAATTGATTGCAGTTGGA-3′) and firefly luciferase (5′-CGTACGCGGAATACTTCGA-3′, luciferase-siRNA), were synthesized by Dharmacon (Lafayette, CO). MDA-MB-231 and MCF7-N55 cells were transfected with Oligofectamine using 20 μg siRNA per 100-mm plate (800,000 cells per plate).

Breast cancer/fibroblast coculture for quantitative PCR. Fibroblasts (early passages 2-9) were plated on the top chamber of a Transwell plate (12-mm-diameter filter, 0.4-μm pore size; Costar, Corning, NY) at a density of 50,000 per well, cultured in complete medium, and starved in serum-free medium (RPMI 1640 with 0.1% BSA) 1 day before start of assay. Breast cancer cells were then seeded on the bottom well of a Transwell system and cocultured in serum-free medium for 5 to 40 hours. For some experiments, breast cancer cells were pretreated with siRNA for Cyr61, PAR1, or luciferase control for 48 hours. Fibroblasts were harvested with PBS/1.5 mmol/L EDTA for RNA extraction.

Isolation of total RNA and quantitative PCR. Total RNA was extracted using the RNeasy mini kit (Qiagen, Valencia, CA). For semiquantitative PCR, 1 μg RNA was reverse transcribed using Moloney murine leukemia virus reverse transcriptase in the presence of deoxynucleotide triphosphate (dNTP; 0.4 μmol/L each). cDNA was amplified in a final volume of 25 μL supplemented with 1.5 mmol/L $MgCl_2$, dNTPs (0.2 μmol/L each) using Taq polymerase (Roche Applied Science, Indianapolis, IN) and the following primers: hMMP-1 sense 5′-CGACTCTAGAAACACAAGAGCAAGA-3′ and antisense 5′-AAGGTTAGCTTACTGTCACACGCTT-3′, mMMP-1 (Mcol-A) sense 5′-TCTTTATGGTCCAGGCGATGAA-3′ and antisense 5′-CCTC-TTCTATGAGGCGGGGATA-3′, and actin sense 5′-GGCTCTTCCAGC-CTTCCTTCCT-3′ and antisense 5′-CACAGAGTACTTGCGCTCAGGAGG-3′. Real-time PCR was conducted in 50 μL volumes containing 1 μL cDNA, 25 μL SYBR Green, 2.5 μL of 5 μmol/L of each of the specific primers and the probe, and 19 μL RNA-free water. All of the reactions were done in triplicate in an iCycle iQ system (Bio-Rad, Hercules, CA). Sequence Detection System 1.9.1 alias program was used in detecting the fluorescent level of MMP-1 and actin for 40 cycles, and the thermal cycling conditions of the Qiagen system were as follows: 15 minutes at 95°C, 30 seconds at 94°C, 1 hour at 55°C, 30 seconds at 72°C, 15 seconds at 95°C, 20 seconds at 55°C, and 15 seconds at 95°C.

Specificity of human and mouse MMP-1 and Cyr61 primers. Total RNA was isolated from CRL-2076 (human) and NIH-3T3 (mouse) and reverse transcribed as described in Materials and Methods. Reverse-transcribed mRNA was PCR amplified using MMP-1-specific primers or actin and visualized by ethidium bromide agarose gel electrophoresis (Supplementary Fig. S1).

Isolation of primary human and mouse mammary fibroblasts. Mammary fat pads were removed from 3- to 6-week-old female wild-type CF-1 mice. Tissue was finely minced with a razor blade as described previously (30). Minced tissue was digested with 10 units/mL collagenase type 1 in RPMI 1640 for 20 minutes at 37°C. The suspension was centrifuged for 10 minutes at 200 × *g* and resuspended in 5 mL RPMI 1640 plus 20% FBS. The resultant culture was confirmed to be fibroblastic by a pathologist. Following approval by the Tufts-New England Medical Center (NEMC) Institutional Review Board, human mammary tissue was obtained from an unidentified female patient who underwent bilateral mastectomy at Tufts-NEMC for removal of an invasive breast adenocarcinoma. Stromal fibroblasts were isolated from human breast tissue as described above.

Western blot analysis. Cells were grown in 100-mm plates and disrupted by multiple passage through a 27-gauge needle in radioimmunoprecipitation assay [RIPA; 150 mmol/L NaCl, 50 mmol/L Tris (pH 8.0), 0.1% SDS, 1% NP40, 0.5% deoxycholate, 1 mmol/L phenylmethylsulfonyl fluoride] and then incubated with heparin beads (Heparin Sepharose 6 Fast Flow, Amersham Pharmacia, Piscataway, NJ) at a ratio of 1:20 (slurry/beads) at 4°C for 1 hour. The beads were washed twice with RIPA containing 400 mmol/L NaCl and eluted with 800 mmol/L NaCl. The eluted lysate was loaded onto 12% polyacrylamide gels and transferred to polyvinylidene difluoride membranes (Immobilion-P, Millipore, Bedford, MA). Soluble Cyr61 from conditioned medium was concentrated 10-fold with Centricon-10 (Millipore). The membrane was incubated with the Cyr61 antibody (0.16 μg/mL) at 4°C for 1 hour. After washing with Tween 20 in TBS, the membrane was then incubated with anti-rabbit Ig-horseradish peroxidase antibody (Dako A/S, Glostrup, Denmark; 1:1,000 dilution) for 1 hour at room temperature. Membrane proteins were detected by enhanced chemiluminescence (Amersham Pharmacia) and exposed on Hyperfilm (Amersham Pharmacia).

Tumor-stromal cell coculturing migration assays. Transwell plates (24-well), with cell culture inserts of 6.5 mm in diameter and 8.0-μm pore size, were used. Fibroblasts were seeded on the bottom wells (100,000 per well) of the Transwell apparatus 2 days before the experiment and starved 1 day before in serum-free medium (RPMI 1640 with 0.1% BSA). Before the experiment, breast tumor cells were resuspended in serum-free medium, plated on the top well (cell culture inserts) at a density of 50,000 (200 μL/well), and allowed to migrate to the underside of the top chamber for 40 hours. The migratory cells attached to the bottom surface of the membrane were stained with Hema 3 Fixative Solution, Hema 3 Solution I, and Hema 3 Solution II (Fisher, Hampton, NH) for 30 seconds at room temperature. Migratory cells in nine randomly selected migratory fields were counted using bright-field microscopy (19). Breast cancer cells or fibroblasts were treated with siRNA and then cocultured. For some experiments, coculture migration assays were also done in the presence of small-molecule ligand-based antagonist of PAR1, RWJ-56110 (31, 32), or aminophenylmercuric acetate–activated MMP-1 (5), which was added to the bottom chamber at the start of assay.

MMP-1 expression and collagenase assay. Collagenase activity was assayed in conditioned medium as described previously (5). Briefly, the cleavage of fluorescein-conjugated 10 μg DQ collagen (Molecular Probes-Invitrogen, Carlsbad, CA) was assayed in 50 mmol/L Tris-HCl (pH 7.6), 150 mmol/L NaCl, 5 mmol/L $CaCl_2$, and NaN_3, and cleavage was monitored continuously over time by a fluorescent microplate reader at 538 nm (excitation at 485 nm) at 25°C. Pro-MMP-1 concentration was determined using Quantikine ELISA (R&D Systems, Minneapolis, MN) according to the manufacturer's instructions.

Statistics. All migration results are presented as mean ± SD. Comparisons were made with Student's *t* test. Statistical significance was defined as $P < 0.05$. SYBR Green I–based quantitative PCR expression levels of target gene transcripts were quantified relative to internal β-actin expression level.

Results and Discussion

PAR1-mediated expression of Cyr61 in breast cancer cells. To test the hypothesis that PAR1 modulates stromal MMP-1 expression through the angiogenic factor Cyr61 (Fig. 1*A*), we first determined whether PAR1 expression and activation induce Cyr61 expression in breast cancer cells. To conduct these studies, we used the PAR1-null breast carcinoma cell line MCF7, which is a poor migratory and nontumorigenic cell line (19) and expresses low basal levels of Cyr61 (26, 33). MCF7 cells were transiently transfected with PAR1 and activated with the strong PAR1 agonist, thrombin. Real-time reverse transcription-PCR (RT-PCR) analyses were used to quantify relative levels of *Cyr61* mRNA. Because *Cyr61* is an early response gene, we predicted that its expression would be rapidly up-regulated. Indeed, treatment of PAR1-expressing MCF7 cells with 1 nmol/L thrombin caused a 3.5-fold up-regulation of *Cyr61* mRNA after 30 minutes with little effect on actin mRNA expression (Fig. 1*B*). Because the transfection frequency was 38%, the 3.5-fold up-regulation is probably an underestimate of PAR1 induction. As a positive control, 17β-estradiol (26, 33) gave a 3-fold induction in *Cyr61* mRNA at the 5-hour time point (Fig. 1*B*).

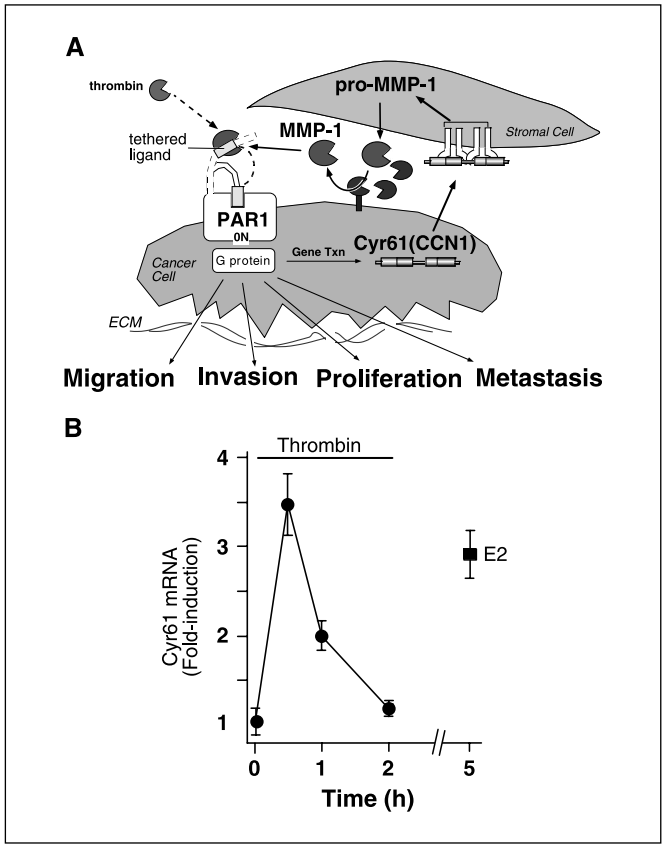

Figure 1. Activation of PAR1 induces *Cyr61* mRNA expression in breast cancer cells. *A,* a model for tumor-derived Cyr61 induction of stromal MMP-1 that results in enhanced tumor cell migration. *B,* MCF7 cells transiently transfected with PAR1 were stimulated with thrombin (1 nmol/L) for 0.5 to 2 hours or 17β-estradiol (*E2*; 100 nmol/L) for 5 hours. Transfection efficiency was 38%. Expression levels of *Cyr61*(*CCN1*) and actin were determined using SYBR Green I–based quantitative PCR. Similar conditions and total amount of RNA were used in each experiment. The relative *Cyr61* gene expression was normalized to the mean value of nonstimulated MCF7 cells transiently transfected with PAR1 (noninduced control), and this value was set to 1. Each of the thrombin-induced time points was divided by the actin control conducted in the identical sample to generate the relative fold induction for *Cyr61*. Experiments were repeated twice. *Points,* mean; *bars,* SD.

Our next approach was to create a series of MCF7 cell lines that stably expressed PAR1 and determine whether PAR1 levels correlated with basal expression of Cyr61 because PAR1 is known to stimulate oncogenic pathways (7, 8) and angiogenesis (9). We generated 21 distinct clones that expressed differing levels of PAR1 on the cell surface. Clone N55 had the highest level of PAR1 expression that was similar to that of MDA-MB-231 cells (19). Clone N26 expressed intermediate levels of PAR1, whereas clone N41 had low or undetectable levels of PAR1 (Fig. 2*A* and *C*). Calcium flux measurements confirmed that PAR1 was activatable by thrombin. As shown in Fig. 2*B*, there was a direct correlation between PAR1 expression levels and the capacity of an individual clone to generate a thrombin-dependent Ca^{2+} signal. There was no thrombin Ca^{2+} signal in the parental MCF7 cells.

PAR1 expression levels have been shown to directly correlate with breast cancer invasion and migration in advanced tumors. We compared different levels of PAR1 expression in the MCF7 parental background and their ability to migrate toward conditioned medium from CRL-2076 fibroblasts. The N55 clone, which expressed the highest levels of PAR1, migrated ~20-fold higher frequency than the parental MCF7 (Fig. 2*C*), which is comparable with the migration rate of the highly invasive MDA-MB-231 cells. Clones N26 and N29, which expressed intermediate levels of PAR1, migrated 10-fold higher than the MCF7 cells. Clones N41 and N50, with undetectable levels of PAR1, migrated at the level of the parental MCF7 cells.

Next, we measured the basal level of Cyr61 expression in each of the clones using Western blot analysis (34) and compared Cyr61 levels with the parental MCF7 cells and with the highly invasive MDA-MB-231 cells, which are known to express high levels of Cyr61 (26). We generated a polyclonal Cyr61 antibody against a peptide corresponding to the unique variable region of Cyr61 (GLLGKELGFDAS-C). Western blot analysis with the affinity-purified Cyr61 antibody detected a specific band at the expected size of 42 kDa in MDA-MB-231 cells that was absent in MCF7 cells (Fig. 2*D*). Interestingly, basal expression of Cyr61 directly correlated with the level of PAR1 expression with high levels of Cyr61 in clone N55, low detectable levels of Cyr61 in clones N29 and N26, and undetectable in clones N50 and 41 (Fig. 2*D*). However, Cyr61 protein has been reported to form high molecular aggregates (35) that may be responsible for the high molecular weight material in lanes N26 and N29. Therefore, to more directly determine whether PAR and Cyr61 expression directly correlate in PAR1-MCF7-derived clones, we measured basal mRNA expression of *Cyr61* and PAR1 (and actin) using quantitative real-time PCR analysis. We then tested whether PAR1 expression would have an effect on *Cyr61* gene expression in the MCF7 clones. Surprisingly, we found a strong correlation ($R = 0.99$; $P < 0.005$) between PAR1 and *Cyr61* expression (Fig. 2*D*). Immunohistochemical staining confirmed that clone N55 expressed high levels of Cyr61 that was secreted into the pericellular space (36) in a pattern similar to that of MDA-MB-231 (Fig. 3*A*; green stain). By comparison, counterstaining for tumor-derived MMP-9 (5) revealed a punctate pattern (red stain) localizing to the cell surface.

Paracrine induction of fibroblast MMP-1 by breast cancer cells. In wound healing models, pure Cyr61 has been shown to

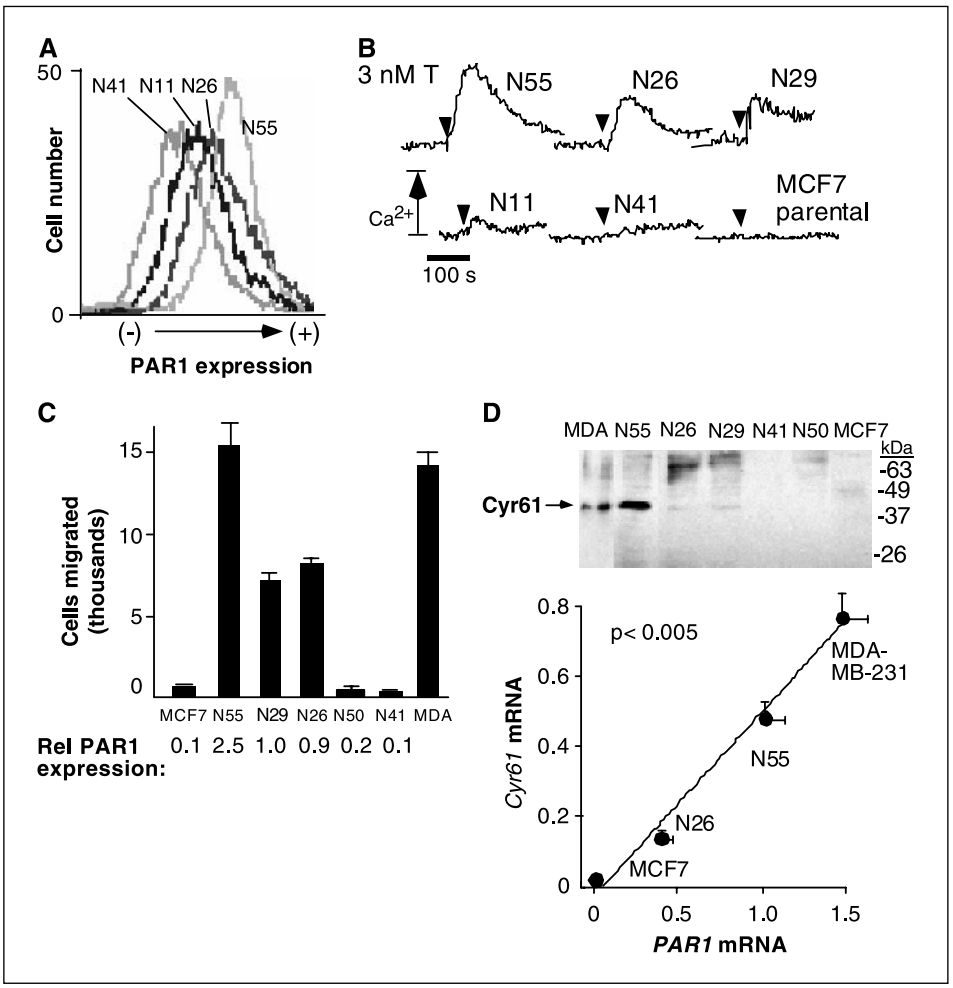

Figure 2. Correlation of PAR1 and Cyr61 expression in stable PAR1-MCF7 cell lines. *A,* PAR1 expression profiles of PAR1-MCF7 clones. Individual PAR1-MCF7 clones (N41, N11, N26, and N55) were labeled with SFLLRN antibody (1 μg/mL), treated with FITC-labeled secondary antibody, and analyzed by flow cytometry. *B,* functional activity of PAR1 in PAR1-MCF7 cell lines. Intracellular calcium fluxes in response to 3 nmol/L thrombin were measured on a Perkin-Elmer (Shelton, CT) LS50B spectrofluorimeter. Cells were labeled with 2.5 μmol/L fura2/AM, and Ca^{2+} fluorescence experiments were done with emission recorded at 510 nm and dual excitation at 340 and 380 nm. *C,* migration of PAR1-MCF7 clones and MCF7 parental cell line toward fibroblast (CRL-2076) conditioned medium. Migration (50,000 cells per top well) was measured in a Transwell apparatus as described previously (19). *D,* correlation of quantitative real-time PCR analysis of the PAR1 and Cyr61 in MCF7, MDA-MB-231, N55, and N26 cells. Cyr61 and PAR1 expression levels were normalized to the reference gene β-actin to correct for variation in the amount of RNA amplified between different cell types. Actin-normalized Cyr61 mRNA levels are plotted on the *Y* axis as a function of normalized PAR1 mRNA levels for MCF7, MCF7-N26, MCF7-N55, and MDA-MB-231 breast cancer cells. Western blot analysis of Cyr61 from extracellular matrix of breast tumor cells. The expression levels of extracellular matrix–bound Cyr61 protein were detected with a polyclonal Cyr61 antibody as described in Materials and Methods.

induce secretion of MMP-1 in fibroblasts (20). Thus, we hypothesized that tumor-derived Cyr61 may have an analogous function in stimulating MMP-1 production from adjacent stromal cells that may contribute to tumor invasion (5). To examine a potential paracrine role of Cyr61, we developed the *in vitro* coculturing model system shown in Fig. 3*B*. WI38 fibroblasts were used as stromal cells in this system because they express low basal levels of Cyr61 (Fig. 3*A*). We compared the high-expressing Cyr61 MDA-MB-231 and MCF7-N55 versus the low-expressing Cyr61 MCF7 breast cancer cells (Fig. 3*A*) for their ability to induce MMP-1 from the WI38 fibroblasts. The MDA-MB-231 or MCF7-N55 cells induced *MMP-1* mRNA expression in WI38 fibroblasts in the coculturing system, whereas MCF7 cells did not (Fig. 3*C*). Using quantitative RT-PCR, we showed that the presence of MDA-MB-231 cells caused a 3.5-fold induction of MMP-1 mRNA in WI38 cells compared with the WI38 cells grown in RPMI 1640 alone (Fig. 3*C*). There was no detectable change in actin mRNA levels. Furthermore, using Western blot analysis, we also confirmed MMP-1 induction at the protein level (Fig. 3*D*). We could detect the expression of both proform (~57/52 kDa) and active forms (42 kDa) of MMP-1 in conditioned medium from cocultured WI38 and MDA-MB-231 cells. There was no detectable MMP-1 in WI38 cells grown alone (Fig. 3*D*). Previously, we have shown that MDA-MB-231 cells do not express MMP-1 (5). Lastly, we used estrogen to transiently induce Cyr61 expression in the MCF7 cells. MCF7 cells grown in estrogen-depleted medium were stimulated with 10 nmol/L β-estradiol and cocultured with WI38 cells. Estrogen stimulation of MCF7 cells caused an induction of *MMP-1* from the WI38 compared with nonstimulated MCF7 control (Fig. 3*C*).

Previous studies (5) showed that mRNA and protein expression levels of MMP-1 were elevated in murine tissues from MCF7-N55 xenografts (7-week-old) compared with control mammary fat pads. To mimic breast cancer cell-stromal cell interactions *in vitro*, we prepared fresh primary mammary fibroblasts from mouse and human tissues. Fibroblasts were used within 7 days of tissue collection without propagation. First, we confirmed that neither the MDA-MB-231 and MCF7-N55 breast cancer cells nor cells from murine mammary fat pads constitutively express MMP-1 (5). Strikingly, there was a strong induction of MMP-1 from the mouse and human mammary stromal fibroblasts in the presence of MCF7-N55 or MDA-MB-231 cells (Fig. 4*A* and *B*). Together, these data indicate that breast cancer cells induce expression of *MMP-1* in primary mammary stromal fibroblasts as occurred with WI38 fibroblasts. These data are consistent with previous observations, which showed that MMP-1 is largely expressed by the surrounding stromal cells recruited to the invasive front of the tumor (4, 37).

Effect of Cyr61 gene silencing on paracrine induction of fibroblast MMP-1. To directly show that breast cancer cells mediate their MMP-1-inducing effects through Cyr61, we silenced *Cyr61* gene expression using Cyr61-siRNA. As shown in Fig. 5*A*, treatment of MDA-MB-231 or MCF7-N55 cells with Cyr61-siRNA

caused a complete loss of Cyr61 expression by Western blot analysis and immunohistochemical staining compared with luciferase-siRNA control. Treatment of the MCF7-N55 cells with Cyr61-siRNA had little effect on expression of the closely homologous CCN family member connective tissue growth factor protein or PAR1 (Fig. 5*B*). Furthermore, treatment of the MCF7-N55 cells with PAR1-siRNA has little effect on expression of Cyr61 protein. Therefore, control of Cyr61 expression becomes independent of PAR1 at some point following the progression of PAR1 oncogenic transformation of MCF7 cells. This may suggest that transcriptional changes late after PAR1 oncogenic induction may result in a new epigenetic control of *Cyr61* gene transcription. Conversely, treatment of the MCF7-N55 cells with Cyr61-siRNA has no effect on PAR1 surface expression. The PAR1-siRNA reduces PAR1 surface expression by 80% at day 2 (these optimal conditions used here) in MDA-MB-231 cells with no effect on the expression of the closely related PAR4 gene (ref. 5; Fig. 1*E*). Furthermore, we showed previously that the PAR1-siRNA treatment did not affect migration of the MDA-MB-231 cells toward IL-8.

To show that tumor cell-derived Cyr61 mediates stromal MMP-1 induction, we cocultured Cyr61-siRNA- or luciferase-siRNA-treated breast cancer cells with WI38 fibroblasts. As shown in Fig. 5*C*, treatment of MCF7-N55 or MDA-MB-231 cells with Cyr61-siRNA

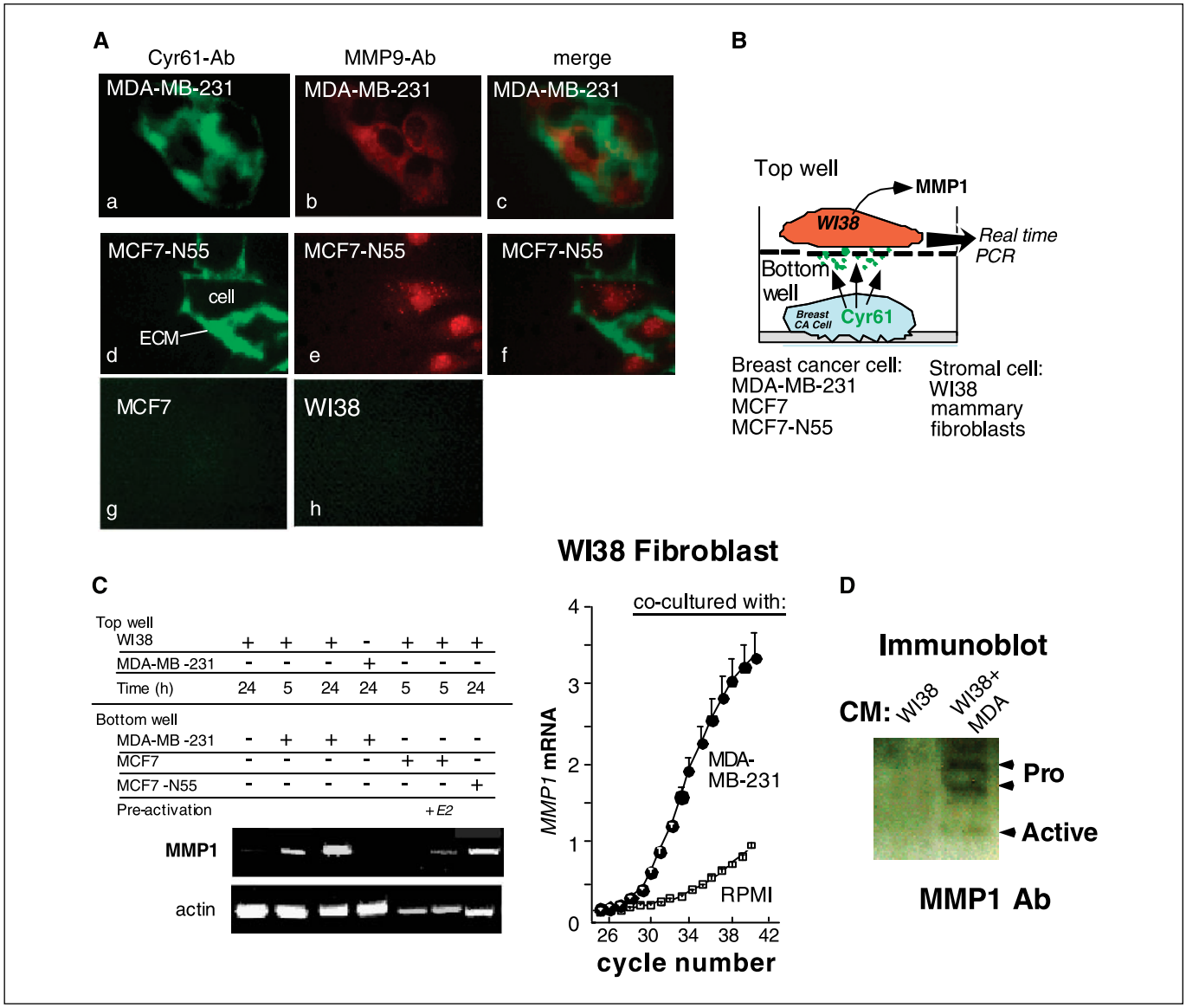

Figure 3. Breast cancer cells induce expression of MMP-1 in fibroblasts. *A,* expression of Cyr61 protein in extracellular matrix of breast tumor cells and fibroblasts. The expression levels of extracellular matrix (*ECM*)–bound Cyr61 protein were detected by immunoblotting analysis using polyclonal Cyr61 antibody. Cells grown on coverslips were stained with anti-human Cyr61 and MMP-9 antibodies, fluorescently labeled, and photographed. Magnification, ×400. Antibody against MMP-9 was used to stain for localization of tumor cells. *B,* schematic representation of coculturing assay for tumor-mediated induction of fibroblast-derived MMP-1. *C,* presence of MDA-MB-231 or MCF7-N55 tumor cells causes induction of *MMP-1* mRNA expression in WI38 cells. RT-PCR of *MMP-1* or actin product was generated using cDNA template isolated from WI38 cocultured with cancer cells. The amplification of actin was carried out to verify that a comparable amount of cDNA was analyzed. Quantitative real-time PCR analysis of *MMP-1* expression in WI38 cells cocultured in the presence of MDA-MB-231 cells for 5 hours. *MMP-1* mRNA expression levels were normalized to the reference gene β-actin to correct for variation in the amount of RNA amplified. Actin-normalized MMP-1 mRNA levels are plotted on *Y* axis as a function of RT-PCR cycle number. *D,* Western blot analysis of conditioned medium from WI38 cells alone or WI38/MDA-MB-231 coculture using MMP-1 antibody (AB806, Chemicon International, Inc., Temecula, CA).

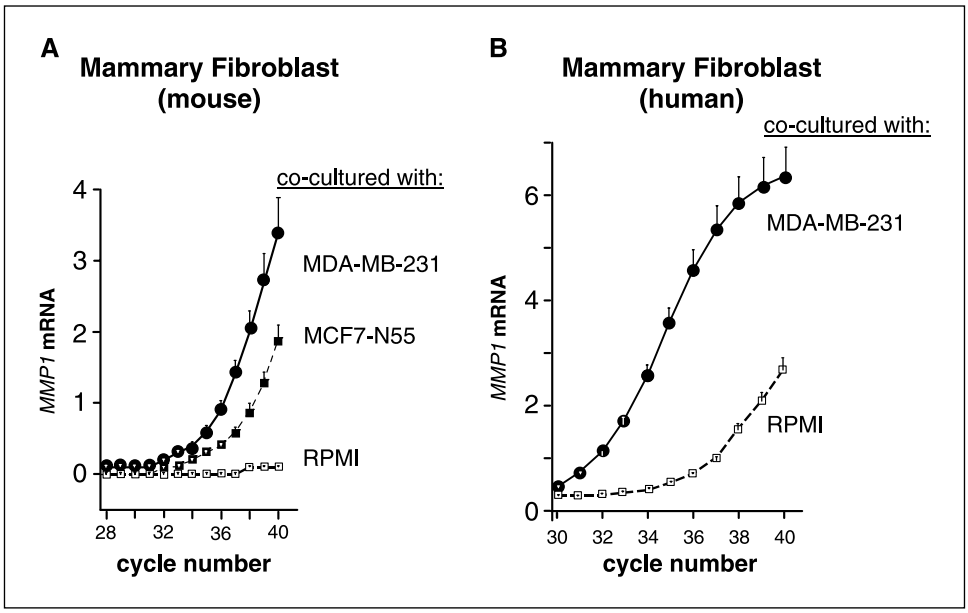

Figure 4. PAR1-expressing breast cancer cells promote MMP-1 production in primary mammary fibroblasts. Primary mouse (*A*) or human (*B*) mammary fibroblasts were cocultured for 20 hours with breast cancer cells MDA-MB-231 or MCF7-N55. MMP-1 mRNA expression levels in the three different fibroblast cells were normalized to the reference gene β-actin to correct for variation in the amount of RNA amplified between different cell types. Actin-normalized MMP-1 mRNA levels are plotted on *Y* axis as a function of RT-PCR cycle number.

caused a 75% to 80% loss of *MMP-1* expression in WI38 cells compared with control cells treated with luciferase-siRNA. These data provide the first direct evidence for the involvement of cancer cell Cyr61 in paracrine regulation of fibroblast MMP-1.

Because MMPs are regulated at the protein level, next we measured MMP-1 levels using Western blot analysis or ELISA and MMP-1 activity using a collagenase assay. As shown in Fig. 3*D*, we found significant paracrine elevation of MMP-1 protein on

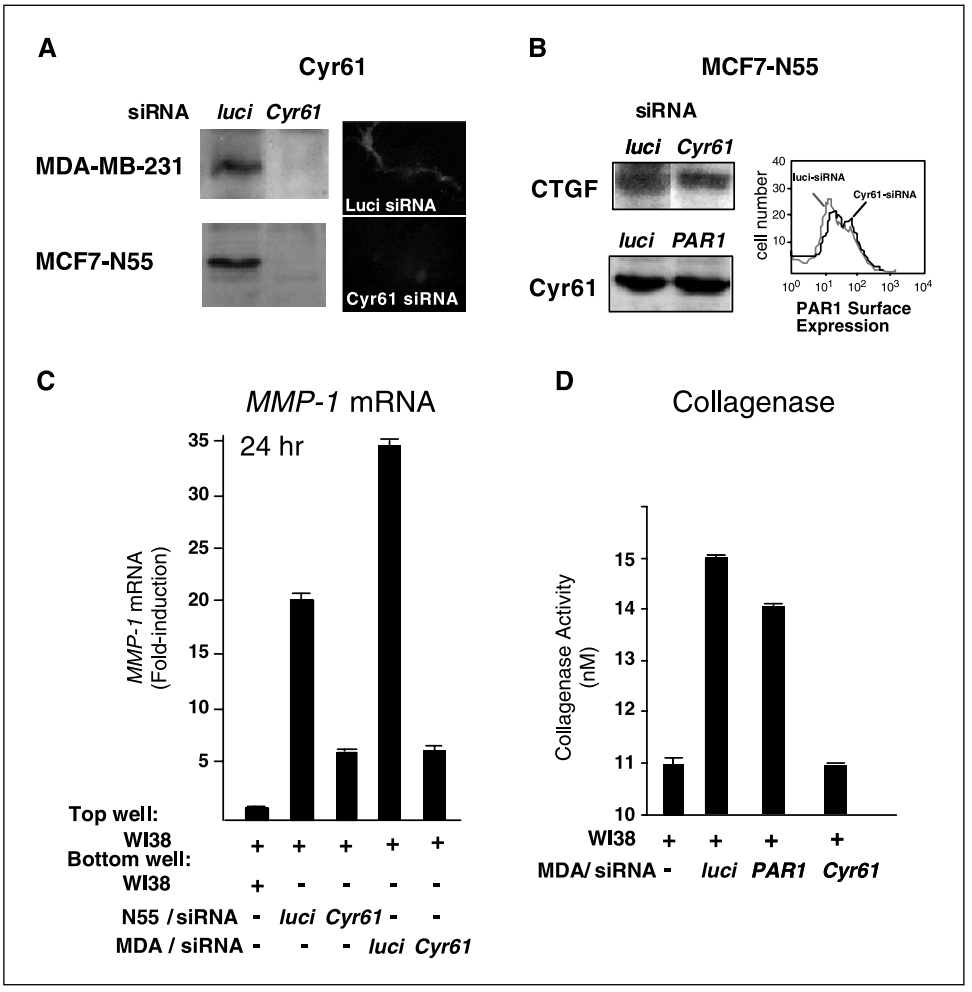

Figure 5. Silencing of Cyr61 in breast cancer cells down-regulates MMP-1 expression levels in fibroblasts. *A,* effect of Cyr61-siRNA on Cyr61 protein expression in MDA-MB-231 or MCF7-N55 cells. Protein was purified using heparin beads, and Western blot analysis was done using the Cyr61 antibody. Immunohistochemical staining using the Cyr61 antibody of luciferase (*luci*)-siRNA- or Cyr61-siRNA-treated MCF7-N55 cells. *B,* effect of Cyr61- and PAR1-siRNA on protein expression of connective tissue growth factor or Cyr61. PAR1 expression profiles of MCF7-N55 treated with Cyr61- or luciferase-siRNA, labeled with SFLLRN antibody (1 μg/mL), and analyzed by flow cytometry. *C,* quantitative real-time PCR analysis of the *MMP-1* expression in WI38 cells cocultured for 24 hours in the presence of MCF7-N55 or MDA-MB-231 cells treated with luciferase- or Cyr61-siRNA. The relative *MMP-1* gene expression was normalized to the mean value of nonstimulated WI38 cells (noninduced control), and this value was set to 1. MMP-1 RT-PCR of each of the siRNA-treated N55 samples was divided by the actin control conducted in the identical sample to generate the relative fold induction for MMP-1. *D,* collagenase activity of conditioned medium from WI38 and MDA-MB-231 cocultures were treated with either luciferase-, PAR1-, or Cyr61-siRNA.

coculturing of WI38 fibroblasts with MDA-MB-231 cells. As expected, we detected expression of predominantly the proform (~57/52 kDa) of MMP-1. As shown in Fig. 5*D*, treatment of MDA-MB-231 cells with Cyr61-siRNA results in ~40% reduction of pro-MMP-1 compared with PAR1- or luciferase-siRNA (from 3.8 ± 0.2 and 4 ± 0.2 to 2.5 ± 0.1 ng/mL) by ELISA. Conversely, coculture with luciferase- or PAR1-treated MDA-MB-231 cells resulted in ~36% increase of collagenase activity. After treatment of MDA-MB-231 cells with Cyr61-siRNA, collagenase activity dropped to basal levels (WI38 cells alone). Together, these data indicate that tumor-derived Cyr61 is directly involved in regulation of stromal MMP-1.

Effect of Cyr61-MMP-1 on migration of cancer cells toward stromal fibroblasts. We tested the ability of WI38 fibroblasts to induce PAR1-dependent chemotaxis of MDA-MB-231 cells. If the paracrine hypothesis is correct, one would predict that gene silencing of Cyr61 in coculturing experiments would give similar effects as silencing PAR1 alone. MDA-MB-231 cells were pretreated with siRNA directed against luciferase, Cyr61, or PAR1 and placed on the top well of the Boyden chamber with WI38 fibroblast cells on the bottom well. The ability of the MDA-MB-231 cells to migrate toward the WI38 cells was then assessed. As shown in Fig. 6*A*, treatment of MDA-MB-231 cells with PAR1-siRNA caused an 80% loss in migration toward WI38 cells. This is consistent with our notion that PAR1 is a major mediator of migration of breast cancer cells as they migrate toward the surrounding stromal fibroblasts (5). Likewise, treatment of MDA-MB-231 cells with Cyr61-siRNA led to a similar 90% loss of migration toward the WI38 fibroblasts compared with luciferase-siRNA control (Fig. 6*A*).

To probe the role of MMP-1 in this tumor-stromal paracrine system, we complemented Cyr61-siRNA-, PAR1-siRNA-, or luciferase-siRNA-treated cells with activated MMP-1. Pro-MMP-1 was first activated with aminophenylmercuric acetate and then dialyzed to remove the cytotoxic mercury compound. As shown in Fig. 6*A* and *B*, Cyr61-siRNA-treated cells, but not PAR1-siRNA-treated MDA-MB-231 or MCF7-N55 cells, could be complemented with 1 nmol/L MMP-1. Furthermore, the regain of migration was completely abrogated by pharmacologic blockade of PAR1 with 1 μmol/L RWJ-56110 (32). As expected, there was no MMP-1-dependent enhancement in migration of PAR1-siRNA-treated MDA-MB-231 or MCF7-N55 cells. Similar results were obtained using either WI38 or human primary mammary stromal fibroblasts (Fig. 6*B*). These data show that the effect of MMP-1 on MDA-MB-231 or MCF7-N55 cell migration toward fibroblasts is PAR1 dependent. Likewise, we showed that coculturing of Cyr61-positive tumor cells with fibroblasts or conditioned medium rescues the defect in migration of Cyr61-siRNA-treated tumor cells (Supplementary Fig. S2). However, tumor PAR1 is essential for this migration process and is not rescued by the Cyr61-positive cells. Together, these results strongly support a paracrine role for tumor-derived Cyr61 in induction of stromal cell MMP-1 that leads to PAR1-dependent cell migration.

Lastly, to confirm that stromal-derived MMP-1 was indeed mediating breast cancer cell migration, we knocked down MMP-1 expression in fibroblasts and cocultured the fibroblasts with breast cancer cells. MCF7-N55 cells were pretreated with siRNA directed against Cyr61, PAR1, or luciferase and placed on the top well of the Boyden chamber with MMP-1-siRNA-treated fibroblasts on the bottom well. As shown in Fig. 6*C*, treatment of fibroblasts with MMP-1-siRNA attenuated 50% chemotaxis of MCF7-PAR1/N55 cells compared with the luciferase-siRNA-treated fibroblasts. The level of inhibition achieved by MMP-1-siRNA treatment of the fibroblasts was similar to that of Cyr61- or PAR1-siRNA treatment of the MCF7-N55 cells. These results confirm that fibroblast-derived MMP-1 mediates migration of these MCF7- or PAR1-expressing cells.

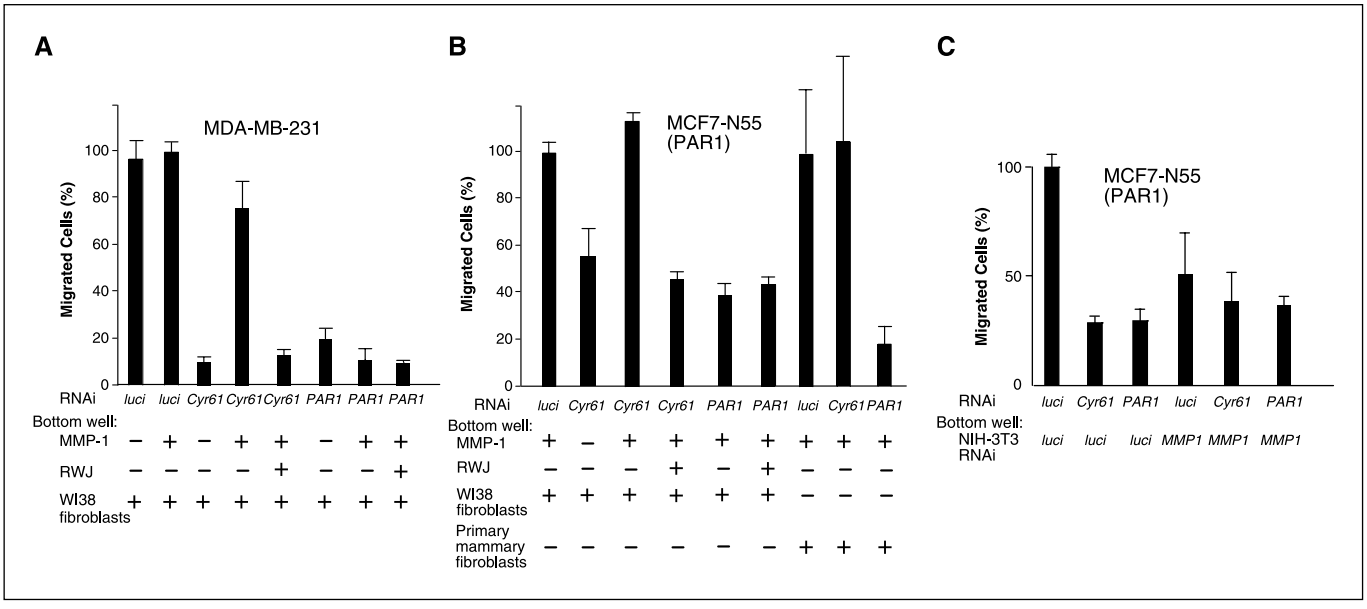

Figure 6. Exogenous MMP-1 complements the Cyr61 defect in PAR1-mediated breast cancer cell migration. *A* and *B,* MDA-MB-231 and MCF7-N55 cells were treated for 48 hours with Cyr61-, PAR1-, or luciferase-siRNA and allowed to migrate toward fibroblasts grown in bottom chamber (100,000 per bottom well) of a Transwell plate in 600 μL RPMI 1640 with 0.1% BSA. Aminophenylmercuric acetate–activated MMP-1 (1 nmol/L) and/or RWJ-56110 (1 μmol/L) was added. *C,* MCF7-N55 (top well) and NIH-3T3 cells (bottom well) were treated for 48 hours with siRNA (Cyr61, PAR1, luciferase-1, or MMP-1). siRNA-treated MCF7-N55 cells (top chamber) were allowed to migrate toward luciferase-siRNA- or MMP-1-siRNA-treated NIH-3T3 cells (bottom chamber) in 600 μL RPMI 1640 with 0.1% BSA. The total number of cells that migrated >40-hour period was counted by microscopy. *Columns,* mean; *bars,* SD.

Conclusions

Cyr61 has been proposed previously to regulate cutaneous wound healing by induction of genes, such as MMPs (20). Matrix remodeling by the MMPs, including interstitial collagenase, MMP-1, is essential for the wound healing process. More recent studies have shown that MMP-1 is marker of poor prognosis in breast, colorectal, and esophageal cancers (1, 2, 38). The PAR1 receptor was identified as an effector molecule for MMP-1 and was found to promote breast cancer cell migration and invasion (5). Here, we present the first evidence that breast cancer cells use Cyr61 to instruct stromal fibroblasts to produce MMP-1, which in turn stimulates PAR1-dependent cancer cell migration. Interestingly, gain-of-constitutive Cyr61 expression was achieved by stably expressing PAR1 in MCF7 cells consistent with findings that PAR1 regulates expression of Cyr61 in fibroblasts (39). These Cyr61-expressing MCF7 cells form tumors that are highly invasive in nude mouse models (5). We show that gene silencing of Cyr61 results in nearly complete inhibition of migration and invasion of breast cancer cells toward stromal fibroblasts. Moreover, it has been shown that forced overexpression of Cyr61 results in a more invasive, tumorigenic MCF7 cell line in the absence of estrogen, and many aggressive breast cancers express high levels of Cyr61 (23, 26, 27). Thus, gain-of-constitutive Cyr61 expression may be an important event in the progression of breast cancer toward a more invasive phenotype.

Acknowledgments

Received 6/14/2005; revised 11/22/2005; accepted 1/9/2006.

Grant support: NIH grants CA104406 (L. Covic), HL64701 (A. Kuliopulos), and HL57905 (A. Kuliopulos) and U.S. Army grant BC045321 (L. Covic).

The costs of publication of this article were defrayed in part by the payment of page charges. This article must therefore be hereby marked *advertisement* in accordance with 18 U.S.C. Section 1734 solely to indicate this fact.

We thank Dr. Sridhar Pal for assistance with fibroblast cultures, Dr. Steve Swift for helpful discussions, Dr. John Erban for his support, and Claudia Derian and Patricia Andrade-Gordon (Johnson and Johnson Pharmaceuticals, Spring House, PA) for providing RWJ-56110.

References

1. Poola I, DeWitty RL, Marshalleck JJ, Bhatnagar R, Abraham J, Leffall LD. Identification of MMP-1 as a putative breast cancer predictive marker by global gene expression analysis. Nat Med 2005;11:481–3.
2. Murray GI, Duncan ME, O'Neil P, McKay JA, Melvin WT, Fothergill JE. Matrix metalloproteinase-1 is associated with poor prognosis in oesophageal cancer. J Pathol 1998;185:256–61.
3. Migita T, Sato E, Saito K, et al. Differing expression of MMPs-1 and -9 and urokinase receptor between diffuse- and intestinal-type gastric carcinoma. Int J Cancer 1999; 84:74–9.
4. Heppner KJ, Matrisian LM, Jensen RA, Rodgers WH. Expression of most matrix metalloprotease family members in breast cancer represents a tumor-induced host response. Am J Pathol 1996;149:273–82.
5. Boire A, Covic L, Agarwal A, Jacques S, Sherifi S, Kuliopulos A. PAR1 is a matrix metalloprotease-1 receptor that promotes invasion and tumorigenesis of breast cancer cells. Cell 2005;120:303–13.
6. Arribas J. Matrix metalloproteases and tumor invasion. N Engl J Med 2005;352:2020–1.
7. Whitehead I, Kirk H, Kay R. Expression cloning of oncogenes by retroviral transfer of cDNA libraries. Mol Cell Biol 1995;15:704–10.
8. Martin CB, Mahon GM, Klinger MB, et al. The thrombin receptor, PAR-1, causes transformation by activation of Rho-mediated signaling pathways. Oncogene 2001;20:1953–63.
9. Yin Y-J, Salah Z, Maoz M, et al. Oncogenic transformation induces tumor angiogenesis: a role for PAR1 activation. FASEB J 2003;17:163–74.
10. Even-Ram S, Uziely B, Cohen P, et al. Thrombin receptor overexpression in malignant and physiological invasion processes. Nat Med 1998;4:909–14.
11. Rudroff C, Seibold S, Kaufmann R, et al. Expression of the thrombin receptor PAR-1 correlates with tumour cell differentiation of pancreatic adenocarcinoma *in vitro*. Clin Exp Metastasis 2002;19:181–9.
12. Nierodzik ML, Chen K, Takeshita K, et al. Protease-activated receptor 1 (PAR-1) is required and rate-limiting for thrombin-enhanced experimental pulmonary metastasis. Blood 1998;92:3694–700.
13. Even-Ram SC, Maoz M, Pokroy E, et al. Tumor cell invasion is promoted by activation of protease activated receptor-1 in cooperation with the $\alpha_v\beta_5$ integrin. J Biol Chem 2001;276:10952–62.
14. Nierodzik ML, Kajumo F, Karpatkin S. Effect of thrombin treatment of tumor cells on adhesion of tumor cells to platelets *in vitro* and metastasis *in vivo*. Cancer Res 1992;52:3267–72.
15. Tellez C, Bar-Eli M. Role and regulation of the thrombin receptor (PAR-1) in human melanoma. Oncogene 2003;22:3130–7.
16. Tellez C, McCarty M, Ruiz M, Bar-Eli M. Loss of activator protein-2α results in overexpression of protease-activated receptor-1 and correlates with the malignant phenotype of human melanoma. J Biol Chem 2003; 278:46632–42.
17. Hazarika P, McCarty MF, Prieto VG, et al. Up-regulation of Flotillin-2 is associated with melanoma progression and modulates expression of the thrombin receptor protease activated receptor 1. Cancer Res 2004; 64:7361–9.
18. Korkola JE, DeVries S, Fridlyand J, et al. Differentiation of lobular versus ductal breast carcinomas by expression microarray analysis. Cancer Res 2003;63: 7167–75.
19. Kamath L, Meydani A, Foss F, Kuliopulos A. Signaling from protease-activated receptor-1 inhibits migration and invasion of breast cancer cells. Cancer Res 2001;61: 5933–40.
20. Chen C-C, Chen N, Lau LF. The angiogenic factors Cyr61 and connective tissue growth factor induce adhesive signaling in primary human skin fibroblasts. J Biol Chem 2001;276:10443–52.
21. Liotta LA, Kohn EC. The microenvironment of the tumour-host interface. Nature 2001;411:375–9.
22. Ito A, Mukaiyama A, Itoh Y, et al. Degradation of interleukin 1β by matrix metalloproteinases. J Biol Chem 1996;271:14657–60.
23. Tsai MS, Hornby AE, Lakins J, Lupu R. Expression and function of CYR61, an angiogenic factor, in breast cancer cell lines and tumor biopsies. Cancer Res 2000;60: 5603–7.
24. Babic AM, Kireeva ML, Kolesnikova TV, Lau LF. CYR61, a product of a growth factor-inducible immediate early gene, promotes angiogenesis and tumor growth. Proc Natl Acad Sci U S A 1998;95:6355–60.
25. Bork P. The modular architecture of a new family of growth regulators related to connective tissue growth factor. FEBS Lett 1993;26:125–30.
26. Xie D, Miller CW, O'Kelly J, et al. Breast cancer. Cyr61 is overexpressed, estrogen-inducible, and associated with more advanced disease. J Biol Chem 2001;276:14187–94.
27. Walter-Yohrling J, Pratt BM, Ledbetter S, Teicher BA. Myofibroblasts enable invasion of endothelial cells into three-dimensional tumor cell clusters: a novel *in vitro* tumor model. Cancer Chemother Pharmacol 2003;52: 263–9.
28. Xie D, Yin D, Tong X, et al. Cyr61 is overexpressed in gliomas and involved in integrin-linked kinase-mediated Akt and β-catenin-TCF/Lef signaling pathways. Cancer Res 2004;64:1987–96.
29. Kuliopulos A, Covic L, Seeley SK, Sheridan PJ, Helin J, Costello CE. Plasmin desensitization of the PAR1 thrombin receptor: kinetics, sites of truncation, and implications for thrombolytic therapy. Biochemistry 1999;38:4572–85.
30. Reiter LA, Rizzi JP, Pandit J, et al. Inhibition of MMP-1 and MMP-13 with phosphinic acids that exploit binding in the S2 pocket. Bioorg Med Chem Lett 1999;9: 127–32.
31. Bernatowicz MS, Klimas CE, Hartl KS, Peluso M, Allegretto NJ, Seiler SM. Development of potent thrombin receptor antagonist peptides. J Med Chem 1996;39:4879–87.
32. Andrade-Gordon P, Maryanoff BE, Derian CK, et al. Design, synthesis, and biological characterization of a peptide-mimetic antagonist for a tethered-ligand receptor. Proc Natl Acad Sci U S A 1999;96:12257–62.
33. Sampath D, Winneker RC, Zhang Z. Cyr61, a member of the CCN family, is required for MCF-7 cell proliferation: regulation by 17β-estradiol and overexpression in human breast cancer. Endocrinology 2001;142:2540–8.
34. Muramatsu Y, Tsujie M, Kohda Y, et al. Early detection of cysteine rich protein 61 (CYR61, CCN1) in urine following renal ischemic reperfusion injury. Kidney Int 2002;62:1601–10.
35. Kireeva ML, Mo FE, Yang GP, Lau LF. Cyr61, a product of a growth factor-inducible immediate-early gene, promotes cell proliferation, migration, and adhesion. Mol Cell Biol 1996;16:1326–34.
36. Yang GP, Lau LF. Cyr61, product of a growth factor-inducible immediate early gene, is associated with the extracellular matrix and the cell surface. Cell Growth Differ 1991;2:351–7.
37. Davies B, Miles DW, Happerfield LC. Activity of type IV collagenases in benign and malignant breast disease. Br J Cancer 1993;67:1126–31.
38. van't Veer LJ, Dai H, van de Vijver MJ, et al. Gene expression profiling predicts clinical outcome of breast cancer. Nature 2002;415:530–6.
39. Pendurthi UR, Allen KE, Ezban M, Rao VM. Factor VIIa and thrombin induce the expression of Cyr61 and connective tissue growth factor, extracellular matrix signaling proteins that could act as possible downstream mediators in factor VIIa tissue factor-induced signal transduction. J Biol Chem 2000;275: 14632–41.

Cell, Vol. 120, 303–313, February 11, 2005, Copyright ©2005 by Elsevier Inc. DOI 10.1016/j.cell.2004.12.018

PAR1 Is a Matrix Metalloprotease-1 Receptor that Promotes Invasion and Tumorigenesis of Breast Cancer Cells

Adrienne Boire,[1,3] Lidija Covic,[1,2] Anika Agarwal,[1] Suzanne Jacques,[1] Sheida Sherifi,[4] and Athan Kuliopulos[1,2,3,*]
[1]Molecular Oncology Research Institute and
[2]Division of Hematology-Oncology
Tufts-New England Medical Center
[3]Department of Biochemistry
Tufts University Medical School
Boston, Massachusetts 02111
[4]Department of Pathology
Mount Auburn Hospital
Cambridge, Massachusetts 02138

Summary

Protease-activated receptors (PARs) are a unique class of G protein-coupled receptors that play critical roles in thrombosis, inflammation, and vascular biology. PAR1 is proposed to be involved in the invasive and metastatic processes of various cancers. However, the protease responsible for activating the proinvasive functions of PAR1 remains to be identified. Here, we show that expression of PAR1 is both required and sufficient to promote growth and invasion of breast carcinoma cells in a xenograft model. Further, we show that the matrix metalloprotease, MMP-1, functions as a protease agonist of PAR1 cleaving the receptor at the proper site to generate PAR1-dependent Ca^{2+} signals and migration. MMP-1 activity is derived from fibroblasts and is absent from the breast cancer cells. These results demonstrate that MMP-1 in the stromal-tumor microenvironment can alter the behavior of cancer cells through PAR1 to promote cell migration and invasion.

Introduction

Protease-activated receptors (PARs) are tethered-ligand receptors that are activated by proteolytic cleavage of their extracellular domains. Four different PARs have been identified: PAR1, PAR2, PAR3, and PAR4 (Coughlin, 2000). PAR1, the prototypic member of the PAR family, has been shown to respond to a highly select group of serine proteases that include thrombin (Vu et al., 1991), plasmin (Kuliopulos et al., 1999), Xa (Riewald et al., 2001), and activated protein C (Riewald et al., 2002). Proteolytic cleavage exposes a new N terminus that binds to the body of the receptor to induce transmembrane signaling to internally located G proteins (Seeley et al., 2003). The activated G proteins in turn trigger a cascade of downstream events, leading to diverse cellular outcomes such as calcium signaling, engagement of integrins, cell adhesion and migration, gene transcription, and mitogenesis.

An emerging common theme is that the PARs act as high-gain sensors of extracellular protease gradients and allow the cell to react to the proteolytically-altered environment. This unique ability to sense proteases can be utilized both for migration toward proteases and for detection of a changing microenvironment (Kamath et al., 2001). More recently, the PARs have been shown to be critically involved in the tissue remodeling processes necessary for normal development including angiogenesis and trophoblastic invasion (Even-Ram et al., 1998; Tsopanoglou and Maragoudakis, 1999; Griffin et al., 2001; Even-Ram et al., 2003; Caunt et al., 2003). Stimulation of PAR1 in atherosclerotic plaques has been implicated in smooth muscle cell proliferation and restenosis and in the response and repair processes of a variety of acute and chronic inflammatory conditions (Nelken et al., 1992).

Beyond its roles in vascular biology and tissue remodeling, PAR1 was identified as an oncogene by its ability to transform NIH-3T3 cells (Whitehead et al., 1995) via Rho pathways (Martin et al., 2001). Ectopic expression of PAR1 in mammary gland epithelia exhibits an oncogenic phenotype of enhanced ductal complexity in mice (Yin et al., 2003). PAR1 has long been proposed to be involved in the invasive and metastatic processes of cancers of the breast, colon, lung, pancreas, prostate, and melanoma (Nierodzik et al., 1992, 1998; Fischer et al., 1995; Even-Ram et al., 1998, 2001; Zain et al., 2000). Even-Ram et al. (1998) demonstrated that PAR1 expression levels were directly correlated with degree of invasiveness in both primary breast tissue specimens and established cancer cell lines. High levels of PAR1 mRNA were found in infiltrating ductal carcinoma and undetectable levels in normal and premalignant hyperplasia. Recent studies by our group (Kamath et al., 2001) showed that the invasive MDA-MB-231 breast cancer cell line expresses very high levels of functional PAR1, PAR2, and PAR4, whereas minimally invasive MCF-7 cells have no PAR1 and low levels of PAR2 and PAR4. Despite the necessity for the presence of functional PAR1 on the cell surface (Even-Ram et al., 1998), neither thrombin nor other serine proteases were shown to be involved in PAR1-dependent breast cancer cell motility, and at high concentrations, thrombin could actually inhibit breast cancer cell invasion (Kamath et al., 2001). Moreover, Zain et al. (2000) had previously shown that thrombin has a bimodal effect on PAR1-dependent growth of melanoma, colon, and prostate carcinomas. Low thrombin concentrations enhance the growth of these cancer cells, whereas high thrombin impairs growth and induces apoptosis. Therefore, a critical issue to be addressed is whether a nonserine protease found in the tumor environment is responsible for the proinvasive properties of PAR1 in the cancer cells.

The most abundant class of nonserine proteases present in invasive and metastatic tumors are the zinc-dependent matrix metalloproteases (MMPs). MMPs are used by invasive cancer cells to hydrolyze the structural proteins that comprise the extracellular matrix such as collagen, elastin, laminin, fibronectin, vitronectin, and fibrinogen (Sternlicht and Werb, 2001). Host

*Correspondence: athan.kuliopulos@tufts.edu

stromal cells also respond to nearby tumor cells by the induction of MMPs (Nelson et al., 2000). Immunohistological examination of human tumor sections revealed that MMPs are largely expressed by the stromal fibroblast and inflammatory cells recruited to the tumor (Heppner et al., 1996).

Here, we show that expression of PAR1 in breast carcinoma cells is sufficient to promote growth and invasion of xenografts in nude mice. We demonstrate that the presence of functional PAR1 accounts for the majority of the invasive signal in breast cancer cells. We identify the matrix metalloprotease, MMP-1, to be a novel protease agonist that cleaves PAR1 at the proper site for receptor activation and generates PAR1-dependent Ca^{2+} signals and migration. Targeting PAR1 with cell-penetrating pepducins can block the pathway downstream of MMP-1 and receptor, inhibiting angiogenesis and cancer growth and invasion.

Results

The Presence of Functional PAR1 Confers Increased Invasion in Breast Cancer Cells

Previous studies by our group (Kamath et al., 2001) and others (Even-Ram et al., 1998) established a correlation between PAR1 expression levels and basal migration of breast cancer cell lines toward conditioned media from NIH-3T3 fibroblasts. We first tested whether the presence of PAR1 is sufficient to confer migration and invasion of breast cancer cells that are normally noninvasive. A PAR1 null breast carcinoma cell line, MCF-7, which has a very low migration index (Kamath et al., 2001), was transfected with either vector alone (pcDEF3) or pcDEF3-PAR1. MCF-7 cells transiently expressing PAR1 exhibited a 3.6-fold increase in migration (Figure 1A) and a 4.3-fold increase in invasion (Figure 1B) through matrigel as compared to their pcDEF3-transfected counterparts. Because simple overexpression of GPCRs can promote constitutive activation of G protein signaling pathways in the absence of agonist, we tested whether a proteolytically dead PAR1 mutant receptor could also confer promigratory behavior to the MCF-7 cells. PAR1 was rendered nonactivatable upon proteolytic cleavage by mutating the tethered ligand residue Phe-43 to alanine. The F43A PAR1 mutant does not transduce a signal to internally located G protein following proteolytic cleavage of the R^{41}-S^{42} bond but fully activates G protein upon addition of exogenous peptide ligand such as SFLLRN or TFLLRN. As shown in Figures 1A and 1B, transfection of MCF-7 cells with F43A PAR1 promoted neither cell migration nor invasion, supporting the hypothesis that PAR1 must be able to be activated for PAR1-dependent migration and invasion to occur.

PAR1 Promotes Tumor Growth and Invasion in Nude Mice

Next, we tested whether the proinvasive phenotype conferred by PAR1 in MCF-7 cells under in vitro conditions could be extended to an in vivo tumor model system. MCF-7 cells are thought to represent an early breast cancer phenotype because they are estrogen-sensitive and require transfection with oncogenes or invasogenic factors to become tumorigenic in nude mice. PAR1 was stably transfected into MCF-7 cells and assessed for the ability to confer tumor growth and invasion in an orthotopic mammary fat pad model in nude mice. Stable MCF7-PAR1 clones were isolated and tested for PAR1 surface expression by FACS. Clone N55 was found to express high levels of PAR1, similar to MDA-MB-231 cells (Kamath et al., 2001), and migrated 16-fold and invaded 30-fold faster through matrigel relative to the parental MCF-7 cells (data not shown). MCF7-PAR1/N55 and the MCF-7 control (PAR1 null) parental cell line were injected into the left and right mammary fat pads, respectively, of female 6- to 7-week-old athymic NCR nu/nu mice (Figure 1C). Tumors developed only in mice injected with MCF7-PAR1/N55 (9/9), and there was no detectable tumor formation with MCF-7 cells (0/10) within 8 weeks (Figure 1D). MCF7-PAR1/N55 tumors grew exponentially in size ranging between 117–268 mm^3 at 6 weeks after injection.

Tumors were excised from the mammary pads 4–10 weeks postinoculation, and hematoxylin and eosin staining of the MCF7-PAR1/N55 breast tumors revealed extensive replacement of normal mammary tissue (see Supplemental Figure S1A in the supplemental data available with this article online). MCF7-PAR/N55 cells formed tumors that were tightly cohesive with poorly differentiated, pleomorphic ductal carcinoma morphology and no recognizable glandular pattern. By 4 weeks, the MCF7-PAR/N55 tumor cells had attached to the abdominal muscle layer. At the 6 week time period, MCF7-PAR1/N55 cells had invaded the adjacent structures including the mammary fat tissue and at 10 weeks had invaded throughout the peritoneal cavity and into the diaphragm (Supplemental Figure S1A). In contrast, there was no detectable tumor formation by the PAR1 null MCF-7 cells, and mammary pads had normal morphology consisting of adipocytes and breast ductules. These data clearly demonstrate that PAR1 can promote tumor growth and invasion in nude mice.

The highly tumorigenic MDA-MB-231 cell line (Kang et al., 2003), which constitutively expresses high levels of PAR1 (Kamath et al., 2001), was also injected into the murine mammary fat pads. Contrary to MCF-7, the MDA-MB-231 cells are estrogen receptor negative and provide a model for more aggressive, tamoxifen-insensitive, breast cancers. MDA-MB-231 cells also have enhanced expression of many genes that are associated with poor outcome in breast cancer patients (van't Veer et al., 2002) and are more likely to form metastases in nude mice models (Kang et al., 2003). Indeed, xenografts formed by MDA-MB-231 (10/10) grew more than 2-fold faster relative to the N55 cells and had already begun to invade into the abdominal muscle wall by week 6 (Figure 1D and Supplemental Figure S1A). We then tested whether knockdown of PAR1 gene expression would affect the mobility of the more invasive MDA-MB-231 breast cancer cells. MDA-MB-231 cells were treated for 48 hr with PAR1 siRNA, then PAR1 surface expression was assessed by FACS. As shown in Figure 1E, treatment of MDA-MB-231 cells with PAR1 siRNA caused an 80% decrease in median surface expression of PAR1 relative to control (luciferase) siRNA-treated cells. The PAR1 siRNA treatment did not perturb surface expression of the PAR4 receptor present

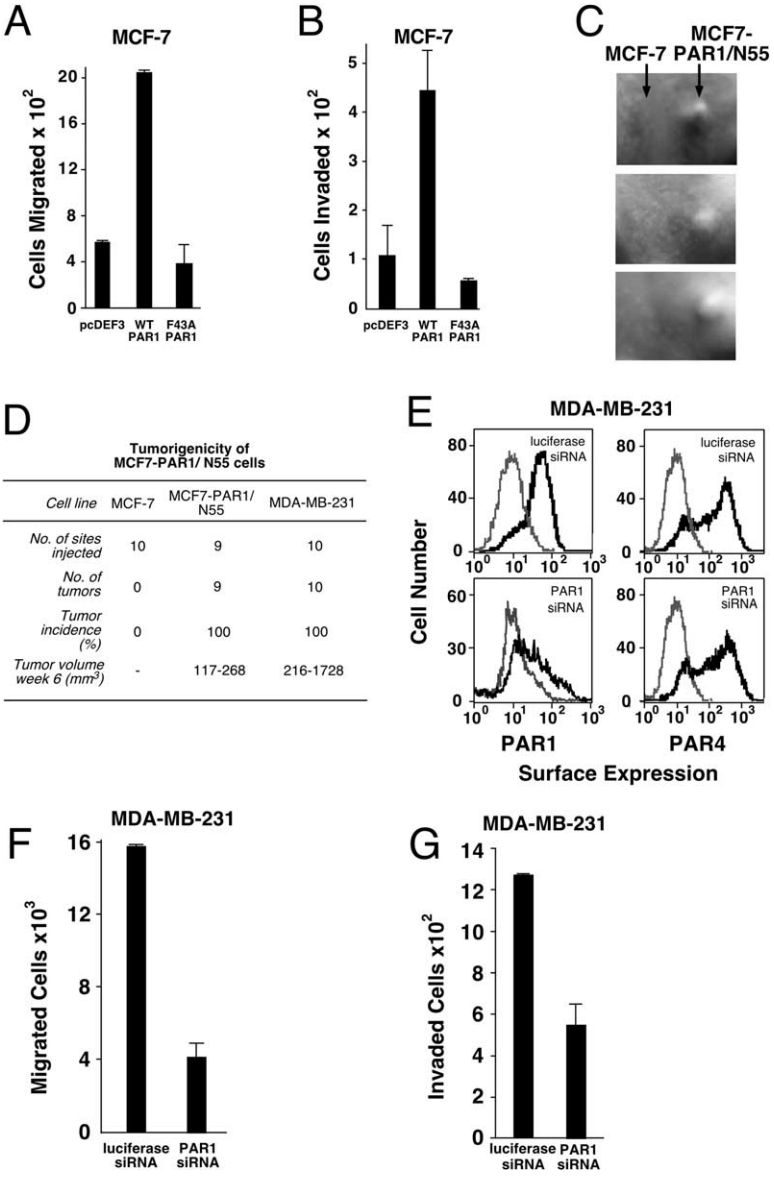

Figure 1. PAR1 Is an Invasogenic Factor in Breast Cancer Cells

(A) Migration of MCF-7 cells transiently transfected with either wt PAR1, a PAR1 mutant (F43A) with a deficient tethered ligand, or vector alone (pcDEF3). MCF-7 cells (50,000) were seeded onto an 8 μm pore membrane in the upper well of a transwell apparatus and allowed to migrate for 5 hr toward conditioned media from NIH-3T3 fibroblasts. Cells that migrated to the lower side of the membrane were counted as described in the Experimental Procedures.

(B) Invasion of transiently transfected MCF-7 cells through 10 μg matrigel per well using NIH-3T3 medium as the chemoattractant source in the bottom well.

(C) Tumor formation of MCF-7 cells (PAR1 null) versus MCF-7 cells stably expressing PAR1 (MCF7-PAR1/N55) inoculated into mammary fat pads of NCR nu/nu mice. Representative tumors shown are from the fourth week postinoculation.

(D) Tumorigenicity of MCF7-PAR1/N55 and MDA-MB-231 breast cancer xenografts.

(E) Silencing of PAR1 expression in MDA-MB-231 cells with PAR1 siRNA versus firefly luciferase siRNA control. Surface expression of PAR1 and PAR4 after 48 hr treatment with siRNA was determined by flow cytometry. Gray traces: secondary antibody alone, Black traces: primary plus secondary antibodies.

(F) Effect of PAR1 siRNA transfection (48 hr) on migration of MDA-MB-231 cells (50,000) toward NIH-3T3 media.

(G) Effect of PAR1 siRNA transfection (48 hr) on invasion of MDA-MB-231 cells (25,000) through matrigel.

on MDA-MB-231 breast cancer cells. Next, we determined the effect of loss of PAR1 expression on the ability of the MDA-MB-231 cells to migrate and invade toward NIH-3T3 medium. As shown in Figures 1F and 1G, the PAR1-siRNA-treated MDA-MB-231 cells migrated 70% less and invaded 60% less through matrigel relative to the control siRNA-transfected counterparts. This 60%–70% loss in migration and invasion as a consequence of the 80% inhibition of PAR1 surface expression suggests that PAR1 may be responsible for the majority of the migratory ability of the MDA-MB-231 cells toward NIH-3T3 media. To provide evidence that the decreased migration response following PAR1 gene silencing is specific to PAR1-mediated events, we tested the effect of PAR1 siRNA treatment on migration toward IL-8, a chemotactic ligand for the CXCR1/2 receptors on MDA-MB-231 cells (Muller et al., 2001). As expected, migration of the MDA-MB-231 cells toward IL-8 was unaffected by the siRNA knockdown of PAR1 relative to untreated control cells (Supplemental Figure S1B).

Matrix Metalloproteases from Fibroblast Media Are Responsible for the Majority of Migration of MDA-MB-231 Breast Cancer Cells

We next sought to determine whether a protease was in fact activating PAR1 and if so, determine the origin of the protease. To address these questions, conditioned medium was prepared from MDA-MB-231 breast cancer cells, NIH-3T3 (murine) immortalized fibroblasts, or CRL-2076 (human) primary fibroblasts. Interestingly, MDA-MB-231 cells migrated about half as well toward their own media as compared to media from the fibroblasts (Figure 2). A panel of protease inhibitors was then assessed for ability to block migration of the MDA-MB-231 cells. Hirudin, a specific thrombin inhibitor, did

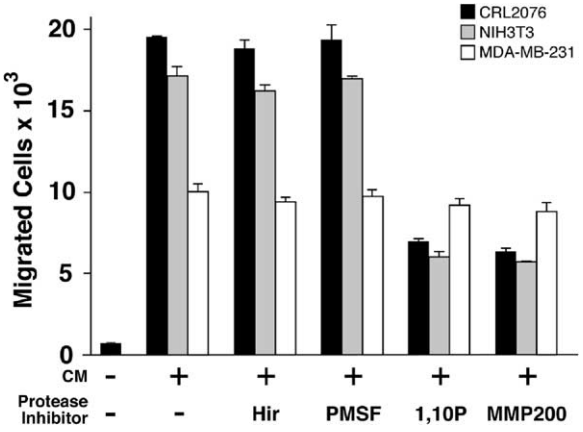

Figure 2. Fibroblast-Derived MMPs Induce Breast Cancer Cell Migration

Migration of MDA-MB-231 breast cancer cells toward either RPMI-1640 (–) or conditioned medium (CM) prepared from primary human CRL-2076 fibroblasts, NIH-3T3 fibroblasts, or MDA-MB-231 cells. The CM was supplemented with the protease inhibitors hirudin (0.015 U), PMSF (100 μM), 1,10-phenanthroline (100 μM + 250 μM $CaCl_2$), MMP-200 (200 nM), or vehicle alone (0.2% DMSO).

not inhibit migration toward any of the media, consistent with previous observations (Kamath et al., 2001). Likewise, addition of the serine protease inhibitor, PMSF, to the media in the bottom well of the chemotactic chambers had no effect on mobility of the MDA-MB-231 cells. These results militate against the direct or indirect participation of serine proteases or thrombin in the migration of the breast cancer cells toward fibroblast or MDA-MB-231 media.

We then turned our attention to another class of proteases which are highly abundant in tumors—namely the Zn^{2+}-dependent matrix metalloproteases. Two broad-spectrum inhibitors of MMPs were employed: 1,10 phenanthroline, a divalent cation-chelating agent, and MMP-200, a hydroxyamate inhibitor of MMPs. Strikingly, the MMP inhibitors reduced the migration of MDA-MB-231 cells toward the fibroblast-derived media by two-thirds (Figure 2). In contrast, the MMP inhibitors did not significantly reduce the migration of MDA-MB-231 cells toward their own medium. Therefore, our data indicate that the MMPs derived from the MDA-MB-231 cancer cells themselves are not sufficient for cell migration. In these in vitro assays, PAR1-dependent migration does not require proteolysis of extracellular matrix; therefore, MMP involvement cannot be attributed to matrix digestion but can be assigned to induction of promigratory signaling pathways in the cells. We hypothesized that MMPs secreted from the fibroblasts were responsible for PAR1 activation and breast cancer cell migration.

PAR1 Activation Induces Promigratory Signaling in MDA-MB-231 Breast Cancer Cells

The MDA-MB-231 cells were treated with a panel of PAR1 antagonists in order to correlate the effects of PAR1 siRNA knockdown with pharmacologic blockade of PAR1. The BMS-200261 and RWJ-56110 compounds are small molecule ligand-based antagonists (Bernatowicz et al., 1996; Andrade-Gordon et al., 1999) that block intramolecular activation of PAR1 by proteolytically generated tethered ligand (Seeley et al., 2003). As shown in Figure 3A, the RWJ-56110 and BMS-200261 compounds blocked up to 57% of the migration of MDA-MB-231 cells toward fibroblast media.

We also determined whether cell-penetrating pepducin antagonists of PAR1 (Covic et al., 2002a; Covic et al., 2002b) could inhibit migration of the MDA-MB-231 cells. The P1pal-12 pepducin is a palmitoylated peptide based on the N-terminal portion of the third intracellular loop (i3) of PAR1 that can interdict signaling between PAR1 and intracellular G proteins. In addition, we tested a C-terminal i3 loop pepducin, P1pal-7, which is a full antagonist of PAR1-G protein signaling (Supplemental Figure S2). As shown in Figure 3A, the P1pal-12 and P1pal-7 pepducins gave similar inhibitory effects as the extracellular PAR1 antagonists RWJ-56110 and BMS-200261 and blocked approximately half of the migration of MDA-MB-231 cells toward fibroblast media.

To further demonstrate that proteolytic activation of PAR1 is capable of stimulating migration of the MDA-MB-231 breast cancer cell line, we inhibited the endogenous MMPs present in the media with MMP-200 and added low concentrations of exogenous thrombin. If it is true that proteolytic activation of PAR1 by an MMP present in the media induces migration, then preventing MMP cleavage of PAR1 should allow activation of PAR1 by exogenous thrombin and recovery of full migration. Indeed, we showed that low concentrations of exogenous thrombin (10–500 pM) can induce full migration of the MDA-MB-231 breast cancer cells. Thrombin induction of MDA-MB-231 cell motility was completely blocked by the BMS-200261 PAR1 antagonist (Figure 3B), thereby demonstrating that the effect of thrombin on the MDA-MB-231 cells was PAR1 dependent. Together, these data suggest that PAR1 activation induced by MMP(s) present in the fibroblast media can be mimicked by exogenous thrombin to cause a major increase in migration of breast cancer cells.

Ability of Individual MMPs to Affect Migration of MDA-MB-231 Breast Cancer Cells

Pure MMPs were tested individually to determine their effects on migration of MDA-MB-231 breast cancer cells. Commercially available pro-MMPs were first activated with aminophenylmercuric acetate (APMA) and then dialyzed to remove the cytotoxic mercury compound. The active form of the MMP was then added to MDA-MB-231 medium placed in the lower well of the chemotactic chamber. Of the MMPs that were tested (MMP-1, -2, -3, -7, and -9), only MMP-1 was able to induce an increase in migration that was nearly equivalent to full migration toward fibroblast-derived media (Figure 4A). Addition of 5 nM MMP-1 to RPMI-1640 serum-free media in the bottom well also induced a significant increase in migration which was completely blocked by the PAR1 antagonist BMS-200261 (Figure 4B).

We knocked down gene expression of PAR1 with siRNA and confirmed that MMP-1 could not act as a chemotactic agent for MDA-MB-231 cells in the ab-

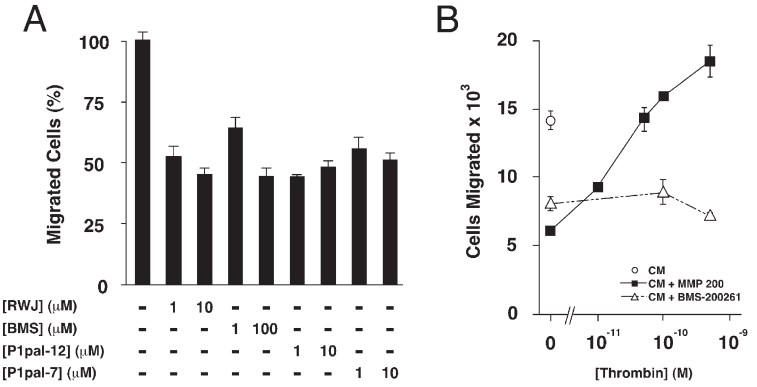

Figure 3. Effect of Inhibition or Stimulation of PAR1 on Migration of MDA-MB-231 Cells

(A) MDA-MB-231 cells migration toward NIH-3T3 CM supplemented with PAR1 antagonists based on either the extracellular ligand (RWJ-56110, BMS-200261) or cell-penetrating pepducins derived from the third intracellular loop of PAR1 (P1pal-12, P1pal-7).

(B) MDA-MB-231 cells migration toward NIH-3T3 CM supplemented with 0–500 pM thrombin in the presence of either MMP-200 (200 nM), BMS-200261 (100 μM), or 0.2% DMSO vehicle (open circle).

sence of PAR1. As shown in Figure 4C, pretreatment of MDA-MB-231 cells with PAR1 siRNA completely blocked MMP1-induced chemotaxis of MDA-MB-231 cells, independently demonstrating that the chemotactic effects of MMP-1 require PAR1. In the converse experiment, we immunodepleted individual MMPs from human CRL-2076 fibroblast media with the corresponding anti-human MMP antibodies coupled to beads. As shown in Figure 4D, immunodepletion of MMP-1 from CRL-2076 media caused a 45% drop in cell migration which accounted for all of the MMP-200-sensitive activity. Treatment of the CRL-2076 media with antibodies directed against MMP-2 or MMP-9 gave slight drops in cell migration. Simultaneous immunodepletion of MMP-1 and MMP-2 gave the same drop in chemotaxis as immunodepletion of MMP-1 alone. No effects were seen upon treatment with anti-MMP-3 or -7 antibodies.

The effect of selective pharmacologic blockade of MMP-1 on cell migration toward NIH-3T3 media was also tested. Three different MMP inhibitors with varying selectivity to MMP-1, MMP-2, and MMP-3 were added to the media in the bottom well. The tetrapeptidyl hydroxamic acid, MMP Inh-1 (FN-439), which targets MMP-1 but not MMP-2 or MMP-3 (Odake et al., 1994), blocked 75% of migration. In contrast, MMP2-Inh (blocks MMP-2) and MMP2/3-Inh (blocks MMP-2 and MMP-3) had no effect on migration of MDA-MB-231 toward NIH-3T3 media. Together, these data demonstrate

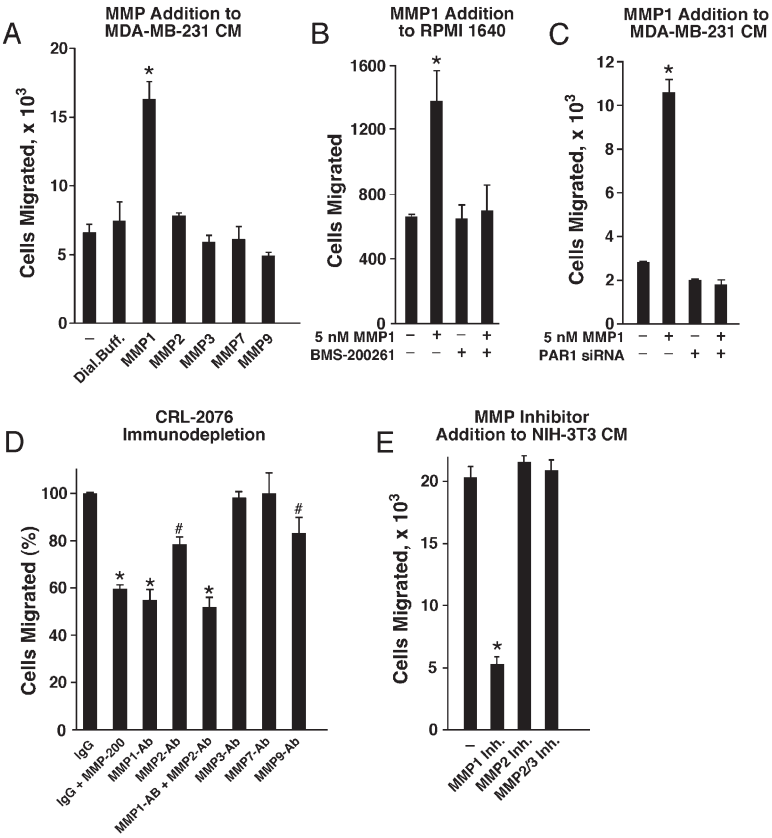

Figure 4. Fibroblast MMP-1 Mediates PAR1-Dependent Migration of Breast Cancer Cells

(A) MDA-MB-231 cell migration toward MDA-MB-231 CM in the presence of 5 nM of APMA-activated MMP-1, MMP-2, MMP-3, MMP-7, MMP-9, or dialysis buffer alone.

(B) MDA-MB-231 migration toward RPMI-1640/0.1% BSA in the presence or absence of MMP-1 and/or the PAR1 antagonist BMS-200261.

(C) MDA-MB-231 cells were treated for 48 hr with PAR1 siRNA or luciferase siRNA control (–) and allowed to migrate toward MDA-MB-231 CM in the presence or absence of MMP-1.

(D) MDA-MB-231 cell migration toward CRL-2076 CM that was immunodepleted for individual MMPs. Monoclonal antibodies against the indicated MMPs or IgG control were coupled to Protein A Sepharose beads and used to immunodeplete CRL-2076 CM. The immunodepleted media served as chemoattractant in a standard migration assay.

(E) MDA-MB-231 cell migration toward NIH-3T3 CM that was supplemented with selective MMP inhibitors used at concentrations $\geq$3-fold above relevant IC_{50}: 3 μM MMP Inh-1 (IC_{50} = 1 μM [MMP-1], 30 μM [MMP-3], 1 μM [MMP-8], 150 μM [MMP-9]), 5 μM MMP2-Inh (IC_{50} = 1.7 μM [MMP-2]), 50 μM MMP2/3-Inh (IC_{50} = 17 μM [MMP-2], 150 nM [MMP-3]). # $p < 0.05$, * $p < 0.01$.

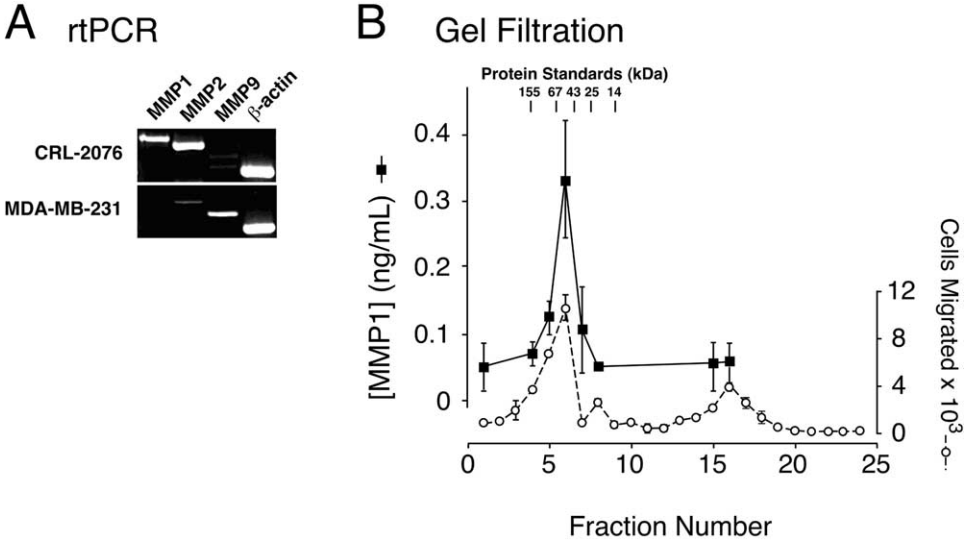

Figure 5. Primary Human CRL-2076 Fibroblasts Secrete MMP-1 into Their Media

(A) CRL-2076 fibroblasts but not MDA-MB-231 breast cancer cells express *MMP-1* mRNA. Total RNA was extracted from CRL-2076 or MDA-MB-231 cells. cDNA was prepared and portions of the cDNA corresponding to *MMP-1*, *MMP-2*, *MMP-9* or *β-actin* messages were amplified by reverse transcriptase PCR and separated on a 1.5% agarose gel.

(B) Serum-free CRL-2076 CM was concentrated 20-fold and 200 μl applied onto a Superose-12 column equilibrated with TBS at 4°C. MMP-1 concentration (mean ± 1 SD; n = 3) was determined in 1 ml fractions by Quantikine ELISA (R&D Systems, Minneapolis). Chemotactic activity of each fraction (dashed line) was determined in duplicate using a standard MDA-MB-231 cell migration assay. This fractionation experiment was repeated three times and gave similar results.

that MMP-1 is capable of inducing PAR1-dependent migration of MDA-MB-231 breast cancer cells and may be responsible for most of the MMP chemotactic activity in the fibroblast media.

Identification of MMP-1 in Media from CRL-2076 Fibroblasts

Using RT-PCR, we confirmed that CRL-2076 fibroblasts express mRNA encoding MMP-1 (Figure 5A). CRL-2076 cells also express mRNA for MMP-2 and very low levels of MMP-9 mRNA. ELISA and collagenase analyses indicated that MMP-1 levels were 34 ± 8 ng/ml (0.6 ± 0.2 nM) and MMP-2 levels were 22 ± 9 ng/ml (0.3 ± 0.1 nM) in the CRL-2076 fibroblast media. Similarly, NIH-3T3 media contained 0.6–1.0 nM MMP-1 collagenase activity. As expected, MDA-MB-231 cells do not have mRNA encoding MMP-1 but do express low levels of MMP-2 mRNA and higher levels of MMP-9 mRNA. The MDA-MB-231 cells did not secrete detectable levels (<0.1 ng/ml) of pro- or active forms of MMP-1 or MMP-2. Together, these data are consistent with other reports which show that MDA-MB-231 cells do not normally express MMP-1 or MMP-2 (Kang et al., 2003).

Extensive studies have shown that breast cancer cells can also migrate toward a variety of small chemokines (0.5–10 kDa) which are abundant in tumor specimens (Youngs et al., 1997; Muller et al., 2001). We next sought to separate the MMP chemotactic activity from the other chemokines potentially secreted by the fibroblasts. Conditioned medium containing fetal bovine serum proved to be exceedingly difficult to fractionate due to the high concentration of albumin. Therefore, we prepared medium from the CRL-2076 fibroblasts under serum-free culture conditions. This serum-free media possessed 85% of the chemoattractive activity of the original CRL-2076 medium for MDA-MB-231 cells. The serum-free CRL-2076 medium was fractionated by size over a Superose-12 gel-filtration column. Individual fractions were assayed for ability to promote migration of the MDA-MB-231 cells. We found that the promigratory activity separated into a major peak (fractions 3–6) and a minor peak (fractions 13–18) (Figure 5B). The chemotactic activity of fractions 3–6 peaked at a relative molecular mass of 55 kDa and together accounted for 55% of the total chemoattractive activity of the loaded material and was blocked by the MMP inhibitor MMP-200 (data not shown). ELISA assays were conducted in order to confirm that MMP-1 was present in the higher molecular mass peak of chemotactic activity. As shown in Figure 5B, MMP-1 eluted at fraction 6, which contained the highest level of chemotactic activity. The small-molecular-mass (<10 kDa) fractions 13–18 contributed to 34% of the total chemotactic activity—in close agreement with the residual chemotactic activity left after treatment of CRL-2076 media with MMP-200 (Figure 2). Thus, the chemotactic activity in fractions 13–18 likely represents small chemokines secreted by the fibroblasts, though this remains to be determined.

MMP-1 Cleaves PAR1 at the Proper Site for Receptor Activation and Generates PAR1-Dependent Ca^{2+} Signals in Breast Cancer Cells

PAR1 is activated by proteolytic cleavage between residues R^{41} and S^{42} which creates a new N terminus, S^{42}FLLRN, that acts as a tethered ligand (Vu et al., 1991; Seeley et al., 2003). To demonstrate that MMP-1 or other MMPs can directly cleave PAR1 at this site, we placed a T7 epitope to the N-terminal side of the

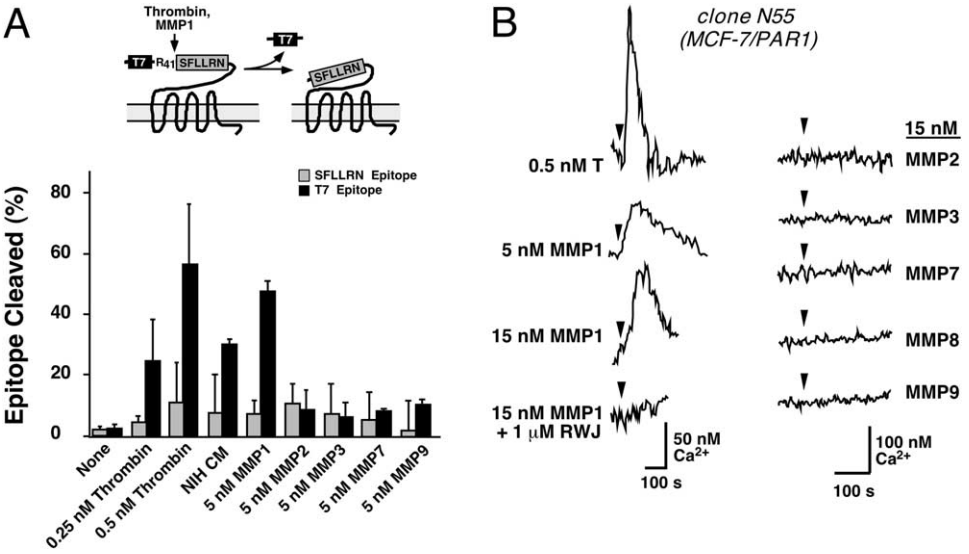

Figure 6. MMP-1 Directly Cleaves PAR1 and Generates PAR1-Dependent Ca^{2+} Signals in Breast Cancer Cells

(A) COS7 cells were transiently transfected with T7-tagged PAR1 incubated with thrombin (T), NIH-3T3 media, or the indicated matrix metalloproteases for 30 min at 37°C. Loss of T7 and SFLLRN epitopes over time (mean ± 1 SD; n = 3) were analyzed by flow cytometry as described (Kuliopulos et al., 1999).

(B) Calcium-flux measurements of MCF7-PAR1/N55 cells following challenge with MMPs or thrombin (T) were performed at 25°C with emission recorded at 510 nm with dual excitation at 340 and 380 nm as described (Kuliopulos et al., 1999).

R^{41}-S^{42} site and expressed the T7-tagged PAR1 in COS7 cells. Cleavage of PAR1 at the R^{41}-S^{42} peptide bond by the MMP would result in loss of the T7 epitope but retention of the SFLLRN epitope (Figure 6A). Indeed, we demonstrated that treatment of the COS7 cells with 5 nM MMP-1 resulted in 50% loss of the T7-epitope while leaving the SFLLRN epitope intact. Similarly, treatment of the T7-PAR1 COS7 cells with 0.5 nM thrombin caused 55% loss of the T7 epitope with retention of the SFLLRN epitope. Treatment with NIH-3T3 media caused 30% loss of the T7 epitope, similar to 0.25 nM thrombin. In contrast, 5 nM concentrations of MMP-2, MMP-3, MMP-7, and MMP-9 gave little cleavage of COS7-expressed T7-PAR1 either to the N- or C-terminal side of the SFLLRN epitope (Figure 6A). These cleavage experiments demonstrate that PAR1 is cleaved at the appropriate site by MMP-1 but is not readily cleaved by MMP-2, -3, -7, or -9.

To directly elicit a functional MMP-1-dependent PAR1 response on the surface of breast cancer cells, we conducted Ca^{2+} flux measurements of the MCF7-PAR1/N55 cells. Addition of 5 nM MMP-1 to N55 cells gave 50% of the Ca^{2+} peak height relative to 0.5 nM thrombin but gave a similar total integrated (area) Ca^{2+} response (Figure 6B). Challenge of the N55 cells with 15 nM MMP-1 gave a robust Ca^{2+} response that was completely blocked by the PAR1-selective antagonist RWJ-56110. None of the other MMPs that were tested (15 nM MMP-2, MMP-3, MMP-7, MMP-8, or MMP-9) were able to elicit a Ca^{2+} signal from the N55 cells.

The Therapeutic Potential of Targeting PAR1 versus MMP-1 on the Growth and Angiogenesis of Breast Tumors

We have demonstrated that the presence of PAR1 promotes tumor growth and invasion; however, we have not yet shown that MMP-1 is also necessary for the tumorigenicity of PAR1-expressing breast cancer cells in vivo. To examine the contribution of MMP-1 to the tumorigenicity of the MCF7-PAR1/N55 cells, we first determined whether the MMP-1 levels were elevated in the N55 tumors relative to control mammary pads. N55 tumors were harvested from untreated mice at week 6 and examined for *MMP-1* mRNA expression and collagenase activity. As shown in Figure 7A, murine *MMP-1* mRNA was induced 2-fold relative to control mammary fat pads. Collagenase activity was enhanced 4-fold in the N55 tumors relative to mammary fat pads (Figure 7B). The collagenase activity in the N55 tumors was inhibited by 50% upon addition of the selective MMP-1 antagonist, MMP Inh-1 (Odake et al., 1994), with no effect on the collagenase activity in the control fat pads, which demonstrates that *MMP-1* expression and MMP-1 collagenase activity are enhanced in the PAR1-expressing N55 breast tumors.

To provide direct evidence that MMP-1 was essential for the tumorigenicity of the PAR1-dependent tumors, we compared the effects of pharmacologic blockade of PAR1 versus MMP-1 on the growth of the N55 breast cancer xenografts. To block PAR1, we used the cell-penetrating i3 loop PAR1 pepducin antagonist, P1pal-7. MCF7-PAR1/N55 cells were injected into the mammary fat pads and the mice treated two days later (to allow implantation) with either vehicle or P1pal-7 (10 mg/kg s.c. every other day) for 6 weeks. As shown Figure 7C, by the 6 week time point, P1pal-7 significantly inhibited (62%) the growth of the MCF7-PAR1/N55 xenografts. The P1pal-7 pepducin treatment was well tolerated by the mice with no observable toxicity. We then treated the mice with MMP Inh-1 for 6 weeks and measured tumor growth. Quite strikingly, MMP Inh-1 treatment of the N55 mice gave 82% inhibition of tumor growth (Fig-

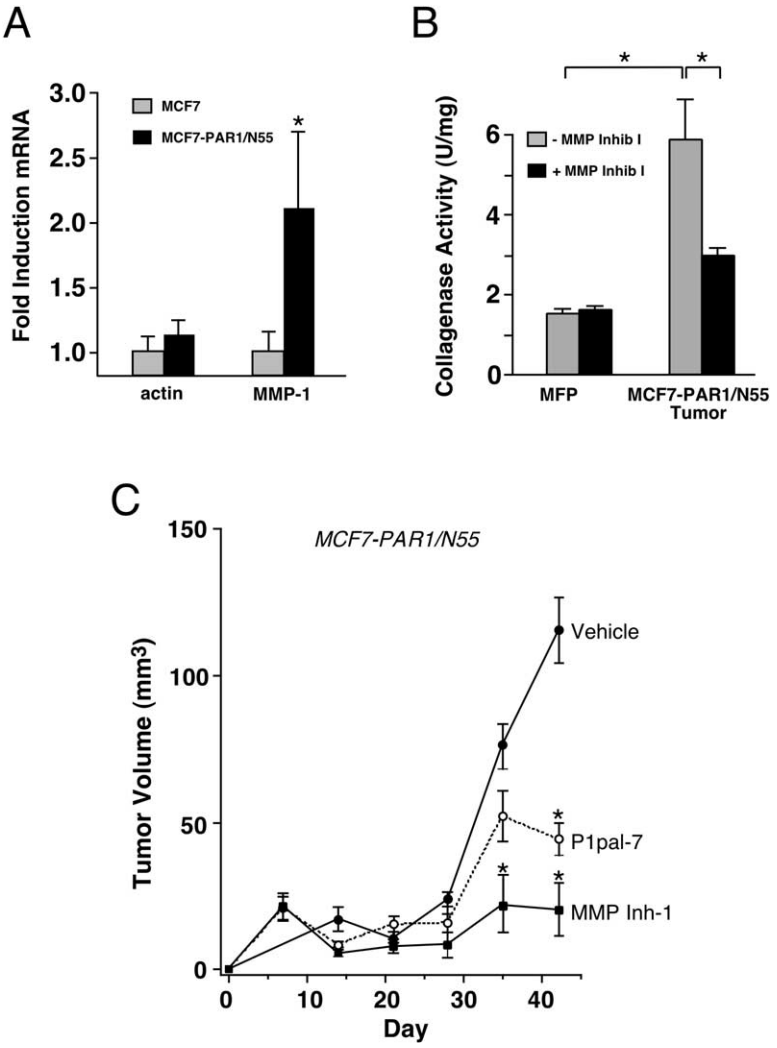

Figure 7. Treatment of Nude Mice with a Cell-Penetrating Pepducin Targeted against PAR1 or an MMP-1 Antagonist Inhibits Growth of Breast Cancer Xenografts

(A) MCF7-PAR1/N55 or MCF-7 cells (4×10^6) were inoculated in the mammary fat pads of NCR nu/nu mice and harvested at 6 weeks. N55 breast tumors or MCF-7 control mammary fat pads were flash frozen in liquid N_2 and tissue disrupted as described in the Experimental Procedures. PCR primers were used to amplify the murine *MMP1A* (Mcol-A) transcript or *actin* control (mean ± 2 SEM; n = 3).

(B) Collagenase activity of the MCF7-PAR1/N55 xenografts or control mammary fat pads (MFP) harvested at 6 weeks was conducted as described in the Experimental Procedures. Collagenase activity was determined in the presence or absence of 5 μM MMP Inh-1 (mean ± 2 SEM; n = 3).

(C) MCF7-PAR1/N55 cells (4×10^6) were inoculated into the mammary fat pads of NCR nu/nu mice. Two days later, treatments (100 μl subcutaneously, every other day) were initiated: (1) vehicle alone (20% DMSO), (2) 10 mg/kg P1pal-7, or (3) 5 mg/kg MMP Inh-1. Tumor volume was measured once weekly using a digital caliper. The median tumor size ± 1 SD, n = 10 breast tumors, is indicated for each data point. * $p < 0.01$.

ure 7C) as compared to untreated control. In in vitro assays, MMP Inh-1 did not nonspecifically block thrombin activity (data not shown). Therefore, these in vivo data provide functional support for the involvement of MMP-1 in the tumorigenesis of human breast cancer cells that express PAR1. These data also indicate that thrombin does not dominate the system and is not able to complement the defect of MMP-1 in the MMP Inh1-treated mice. It still remains possible that MMP-1 plays other roles beyond cleavage and activation of PAR1 in these tumors.

Lastly, we compared the morphology, invasive edge, and degree of vascularization of the untreated (vehicle) versus P1pal-7- and MMP Inh-1-treated N55 breast tumors harvested at the end of the experiment of Figure 7C. Hematoxylin and eosin staining showed that the morphology of the N55 tumors from all three groups was similar to poorly differentiated invasive ductal carcinoma of human breast specimens. The xenografts from the P1pal-7 and MMP Inh-1 treatment groups gave a very similar infiltrating pattern of tumor growth into the adjacent skeletal muscle (Supplemental Figure S3). Immunohistochemical staining for endothelial cells revealed prominent von Willebrand Factor-positive vascular structures within the central tumor mass of the untreated group. In contrast, significantly less vascularity was present in the Plpal-7- and MMP Inh-1-treated groups (Supplemental Figure S3). Therefore, P1pal-7 and MMP Inh-1 treatment have the same effects on tumor morphology, invasion, and vascularity. Furthermore, these results are consistent with the proposed role of PAR1 in angiogenesis (Griffin et al., 2001; Yin et al., 2003; Caunt et al., 2003) and provide evidence that MMP-1 may also promote angiogenesis by activating PAR1.

Discussion

The present study made the unanticipated discovery that PAR1 can be directly activated by the interstitial collagenase MMP-1. Although several serine proteases have been identified as PAR agonists, this is the first report that a PAR can be activated by a member of the zinc-dependent matrix metalloprotease family. PAR1 activation by MMP-1 provides a link between extracellular proteolytic activity important for remodeling of the

extracellular matrix with signaling leading to cell migration and invasion.

We also showed that PAR1 is a potent tumorigenic and invasogenic factor for human MCF-7 breast cancer cells in an orthotopic nude mouse model. PAR1 expression has been directly correlated with degree of invasiveness in both primary breast tissue specimens (Even-Ram et al., 1998) and in established cancer cell lines from humans (Nierodzik et al., 1998; Ross et al., 2000). Similarly, MMP-1 has been shown to be a marker of poor prognosis in breast, colorectal, and esophageal tumors (Murray et al., 1998; van't Veer et al., 2002).

As a new example of tumor-host interdependence, we showed that the MMP-1 that was cleaving PAR1 was not produced by the breast cancer cells themselves but instead was secreted by the fibroblasts. Indeed, overwhelming evidence suggests that MMPs necessary for the invasion of cancer cells originate mainly from stromal fibroblasts, myofibroblasts, inflammatory cells, and endothelium (Egeblad and Werb, 2002). Immunohistological examination of human tumor sections revealed that MMP-1 and other MMPs are expressed by the stromal cells recruited to the tumor (Heppner et al., 1996; Nelson et al., 2000). The tumor cells secrete several factors including interleukins, cytokines, and angiogenesis factors, to induce the host stromal cells to produce MMPs (Zucker et al., 1998; Nelson et al., 2000, Sternlicht and Werb, 2001). Conversion of fibroblast-derived pro-MMP-1 to active MMP-1 by membrane-tethered or membrane-associated MMPs may present high local concentrations of MMP-1 to PAR1 on the same tumor cell surface.

We showed that the endogenous MMP-1 activity generated in situ from the fibroblast media cleaves PAR1 and is sufficient to cause robust migration and invasion of breast cancer cells via PAR1. Indeed, MMP-1 cleavage of PAR1 compares favorably with factor Xa (Camerer et al., 2000), plasmin (Kuliopulos et al., 1999), and activated protein C (APC) (Riewald et al., 2002) activation of PAR1 relative to thrombin. To our knowledge, we have provided the first demonstration of direct activation of a G protein-coupled receptor by an MMP.

A biological rationale for our results is that the breast cancer cells first utilize fibroblast-derived MMP-1 to activate PAR-1 which promotes cell migration toward the stroma and MMP-1 source. MMPs derived from the cancer cell itself or adherent to the cancer cell may help to catalyze activation of pro-MMP-1 and digest the ECM at the invasion front and together with the MMP1-PAR1 chemotactic signal allow the cell to invade into the surrounding stromal tissues. During the later vascular invasive and metastatic stage when the cancer cells acquire the ability to enter the blood stream, PAR1 may be activated by the TF-thrombin system and help mediate adhesion to the endothelium and underlying matrix at distant metastatic sites, perhaps with the assistance of adherent platelets (Nierodzik et al., 1992; Fischer et al., 1995). It is possible that MMP-1 may also play a role in the later metastatic phase of breast cancer progression. Interestingly, Kang et al. (2003) showed that bone metastases originating from MDA-MB-231 fat pad xenografts have enhanced MMP-1 expression. Therefore, depending on the relative local concentrations of MMP-1 and thrombin and the stage of tumor progression, either protease could activate PAR1-dependent signaling to cause the cancer cell to migrate, invade, or adhere.

Another area where MMPs and PARs have both been shown to play important roles is in inflammation and atherosclerosis (Nelken et al., 1992; Libby and Aikawa, 2002). Increased expression of MMP-1 and other MMPs occurs in the vulnerable shoulder and cap regions of atherosclerotic plaques (Libby and Aikawa, 2002). MMP-1, which is expressed in the macrophages, vascular smooth muscle cells, and endothelium of atheromatous plaques, is the most abundant MMP present that can cleave the native collagen types I and III which comprise the major tensile components of the fibrous plaque cap (Libby and Aikawa, 2002). Therefore, it has been suggested that MMP-1 may be partly responsible for plaque rupture. Stimulation of PAR1 in atherosclerotic plaques has also been implicated in smooth muscle cell proliferation and restenosis and exaggerated vasoconstrictory response (Nelken et al., 1992; Ku and Dai, 1997). It has been assumed that thrombin is the agonist that is activating PAR1-dependent proinflammatory and proliferative signaling within the atherosclerotic plaque; perhaps MMP-1 may contribute to PAR1 activation in the inflammatory lesion.

Finally, our results, together with the foregoing studies, suggest that therapeutics that block MMP-1 may prove beneficial in the treatment of a variety of invasive, proliferative, and inflammatory conditions. However, numerous phase III clinical trials with broad-spectrum MMP inhibitors for treatment of diverse cancers have suffered from dose-limiting joint toxicity thought to be due to inhibition of MMP-1 (Nelson et al., 2000; Yamamoto et al., 2002). Hence, PAR1, a new receptor for MMP-1, becomes an attractive target as a novel therapeutic approach, as exemplified by the PAR1 pepducin P1pal-7, for blocking the progression and angiogenesis of invasive and metastatic cancers and in inflammatory conditions when it is not possible to directly inhibit MMP-1.

Experimental Procedures

Reagents

Recombinant hirudin and purified human MMPs were obtained through EMD Biosciences (San Diego, California). MMP-200 was from Enzyme Systems Products (Livermore, California). MMP Inh-I, MMP2-Inh, and MMP2/3-Inh were from Calbiochem (La Jolla, California). BMS-200261 was synthesized by AnaSpec (San Jose, California). N-palmitoylated peptides P1pal-12 and P1pal-7 were synthesized by standard fmoc solid phase synthetic methods with C-terminal amides as before (Covic et al., 2002a). Rabbit polyclonal PAR1-Ab and PAR4-Ab were purified by peptide affinity chromatography as described previously (Kuliopulos et al., 1999).

Molecular Biology

Construction of the genes encoding human PAR1 have been described (Kuliopulos et al., 1999; Jacques and Kuliopulos, 2003). A PAR1 mutant with a deficient tethered ligand, F43A, was constructed as described (Chen et al., 1994). All PAR1 constructs were inserted into the mammalian expression vector pcDEF3, which places PAR1 under the control of a human EF-1a promoter and carries a neomycin selectable marker. Small interfering (si)-RNA directed against PAR1 (5′-AAGGCUACUAUGCCUACUACU-3′), and firefly luciferase (5′-CGTACGCGGAATACTTCGA-3′) were synthesized by Dharmacon (Lafayette, Colorado). For rt-PCR, total RNA was extracted from MDA-MB-231 and CRL-2076 cells with the

Rneasy mini kit (Qiagen, Valencia, California). cDNA was prepared with 5 μg of total RNA using MMLV reverse transcriptase. The desired products were amplified with Taq polymerase and the following primers: hMMP-1 sense 5′-CGACTCTAGAAACACAAGA GCAAGA-3′, antisense 5′-AAGGTTAGCTTACTGTCACA CGCTT-3′; hMMP-2 sense 5′-GTGCTGAAGGACACACTAAAGAAGA-3′, antisense 5′-TTGCCATCCTTCTCAAAGTTGTAGG-3′; hMMP-9 sense 5′-CACTGTCCACCCCTCAGAGC-3′, antisense 5′-GCCACTTGTCG GCGATAAGG-3′; mMMP-1 (Mcol-A) sense 5′-TCTTTATGGTCCA GGCGATGAA-3′, antisense 5′-CCTCTTCTATGAGGCGGGGATA-3′.

Cell Culture

MDA-MB-231 and MCF-7 cells (human breast carcinomas) were obtained from the NCI (Frederick, Maryland). NIH-3T3 and CRL-2076 fibroblasts were from the ATCC (Manassas, Virginia). MCF-7 cells were transfected using LipofectAMINE, and 20 μg of DNA were used for each 100 mm tissue culture dish. MCF-7 cells stably expressing wt PAR1 such as clone N55 (MCF7-PAR1/N55) were first selected with 750 μg/ml geneticin for one week and then retrieved with magnetic Dynabeads (M450) coupled with the PAR1-Ab. MDA-MB-231 cells were transfected with OligofectAMINE using 20 μM siRNA oligo per 100 mm plate.

Conditioned Media Preparation and Migration and Invasion Assays

MDA-MB-231, NIH-3T3, or CRL-2076 cells were growth to 50% confluency. The media was then changed to fresh growth media and cells were incubated for an additional 48 hr. The conditioned media was drawn off the cells and centrifuged at 25°C for 5 min at 200 × g to remove debris and stored at −20°C. Invasion of cells through matrigel was conducted using a Transwell apparatus (Corning Costar) as described previously (Kamath et al., 2001). Data is expressed as mean number of cells migrating ±1 SEM (n = 2–4).

Orthotopic Mammary Fat Pad Model in Nude Mice

These experiments were conducted in full compliance with the Tufts-NEMC Institutional Animal Care and Use Committee. Groups of five NCR nu/nu mice (Taconic Farms) each received two mammary fat pad inoculations consisting of 4×10^6 MCF-7 and 4×10^6 MCF7-PAR1/N55 human breast cancer cells. Tumors and surrounding tissue were excised from sacrificed mice, fixed in 10% formalin/PBS, and imbedded in paraffin. Tissue sections (5 μm) were prepared and stained with hematoxylin-eosin.

MMP-1 Expression and Collagenase Activity

Breast tumor xenografts or control mammary fat pads were excised from nude mice, and tissue samples were lysed by freezing the tissue in liquid nitrogen, grinding the frozen tissue to a powder, and adding the powder to lysis buffer. The lysis buffer consisted of RNeasy lysis buffer (Qiagen) for RT-PCR and 10 mM Tris-HCl (pH 7.4), 150 mM NaCl, 1 mM $CaCl_2$, 1 mM $MgCl_2$, 0.1% Triton X-100, 100 μM PMSF, 100 mM dithiothreitol, and 10 μg/ml leupeptin for the collagenase assay. Collagenase activity was assayed in lysed tumor samples and in fibroblast media by measuring the cleavage of fluorescein conjugated DQ collagen (Molecular Probes). Collagenase assays contained 10 μg DQ collagen in 50 mM Tris-HCl (pH 7.6), 150 mM NaCl, 5 mM $CaCl_2$, and 0.2 mM NaN_3, and cleavage was monitored continuously over time by a fluorescence microplate reader at 538 nm (excitation at 485 nM) at 25°C. One unit of collagenase activity was defined as the cleavage of 1 μg collagen per minute at 25°C.

Activation of pro-MMPs

Stock solutions of pro-MMPs containing 400 nM pro-MMPs were activated with 2 mM APMA in 50 mM Tris (pH 7.7), 5 mM $CaCl_2$, 0.2 M NaCl, and 50 μM $ZnCl_2$ at 37°C for 30 min and then transferred to an ice bath prior to use. For migration assays, the APMA was removed by overnight dialysis in 10 kDa MWCO Mini Slide-A-Lyzers (Pierce, Rockford, Illinois) at 4°C.

Immunodepletion of MMPs

CRL-2076-conditioned medium was diluted 1:3 with 20 mM potassium phosphate buffer (pH 7.5), 150 mM NaCl (PBS) (1.3 ml final volume), and 5 μg MMP-Ab or IgG control was added and the mixture and gently rocked at 4°C for 2 hr. Antibody-antigen complexes were bound to Protein A beads (Pharmacia, Piscataway, New Jersey) (130:5 v/v) by incubating for an additional 2 hr. The Protein A-antibody/antigen beads were removed from the medium by centrifugation (300 × g for 5 min, 4°C).

Supplemental Data

Supplemental Data include three figures and can be found with this article online at http://www.cell.com/cgi/content/full/120/3/303/DC1/.

Acknowledgments

This work was funded in part by a predoctoral fellowship from the Susan G. Komen Breast Cancer Foundation (A.B.) and by NIH grant HL64701 (A.K.). We are especially grateful for the expert advice and support of John Erban. We thank Claudia Derian and Patricia Andrade-Gordon of Johnson and Johnson Pharmaceuticals for providing RWJ-56110 and Nga Nguyen for conducting the RT-PCR analyses and Richard Wong for conducting the IL-8 migration assays.

Received: April 15, 2004
Revised: November 9, 2004
Accepted: December 6, 2004
Published: February 10, 2005

References

Andrade-Gordon, P., Maryanoff, B.E., Derian, C.K., Zhang, H.-C., Addo, M.F., Darrow, A.L., Eckardt, A.J., Hoekstra, W.J., McComsey, D.F., Oksenberg, D., et al. (1999). Design, synthesis, and biological characterization of a peptide-mimetic antagonist for a tethered-ligand receptor. Proc. Natl. Acad. Sci. USA *96*, 12257–12262.

Bernatowicz, M.S., Klimas, C.E., Hartl, K.S., Peluso, M., Allegretto, N.J., and Seiler, S.M. (1996). Development of potent thrombin receptor antagonist peptides. J. Med. Chem. *39*, 4879–4887.

Camerer, E., Huang, W., and Coughlin, S.R. (2000). Tissue factor- and factor X-dependent activation of protease-activated receptor 2 by factor VIIa. Proc. Natl. Acad. Sci. USA *97*, 5255–5260.

Caunt, M., Huang, Y.-Q., Brooks, P.C., and Karpatkin, S. (2003). Thrombin induces neoangiogenesis in the chick chorioallantoic membrane. J. Thromb. Haemost. *1*, 2097–2102.

Chen, J., Ishii, M., Wang, L., Ishii, K., and Coughlin, S.R. (1994). Thrombin receptor activation. J. Biol. Chem. *269*, 16041–16045.

Coughlin, S.R. (2000). Thrombin signalling and protease-activated receptors. Nature *407*, 258–264.

Covic, L., Gresser, A.L., Talavera, J., Swift, S., and Kuliopulos, A. (2002a). Activation and inhibition of G protein-coupled receptors by cell-penetrating membrane-tethered peptides. Proc. Natl. Acad. Sci. USA *99*, 643–648.

Covic, L., Misra, M., Badar, J., Singh, C., and Kuliopulos, A. (2002b). Pepducin-based intervention of thrombin receptor signaling and systemic platelet activation. Nat. Med. *8*, 1161–1165.

Egeblad, M., and Werb, Z. (2002). New functions for the matrix metalloproteinases in cancer progression. Nat. Rev. Cancer *2*, 161–174.

Even-Ram, S., Uziely, B., Cohen, P., Grisaru-Granovsky, S., Maoz, M., Ginzburg, Y., Reich, R., Vlodavsky, I., and Bar-Shavit, R. (1998). Thrombin receptor overexpression in malignant and physiological invasion processes. Nat. Med. *4*, 909–914.

Even-Ram, S.C., Maoz, M., Pokroy, E., Reich, R., Katz, B.-Z., Gutwein, P., Altevogt, P., and Bar-Shavit, R. (2001). Tumor cell invasion is promoted by activation of protease activated receptor-1 in cooperation with the alpha v beta 5 integrin. J. Biol. Chem. *276*, 10952–10962.

Even-Ram, S.C., Grisaru-Granovsky, S., Pruss, D., Maoz, M., Salah, Z., Yong-Jun, Y., and Bar-Shavit, R. (2003). The pattern of expres-

sion of protease-activated receptors (PARs) during early trophoblast development. J. Pathol. *200*, 47–52.

Fischer, E.G., Wolfram, R., and Mueller, B.M. (1995). Tissue factor-intiated thrombin generation activates the signaling thrombin receptor on malignant melanoma cells. Cancer Res. *55*, 1629–1632.

Griffin, C.T., Srinivasan, Y., Zheng, Y.-W., Huang, W., and Coughlin, S.R. (2001). A role for thrombin receptor signaling in endothelial cells during embryonic development. Science *293*, 1666–1670.

Heppner, K.J., Matrisian, L.M., Jensen, R.A., and Rodgers, W.H. (1996). Expression of most matrix metalloprotease family members in breast cancer represents a tumor-induced host response. Am. J. Pathol. *149*, 273–282.

Jacques, S.L., and Kuliopulos, A. (2003). Protease-activated receptor-4 uses dual prolines and an anionic recognition motif for thrombin recognition and cleavage. Biochem. J. *376*, 733–740.

Kamath, L., Meydani, A., Foss, F., and Kuliopulos, A. (2001). Signaling from protease-activated receptor-1 inhibits migration and invasion of breast cancer cells. Cancer Res. *61*, 5933–5940.

Kang, Y., Siegel, P.M., Shu, W., Drobnjak, M., Kakonen, S.M., Cordon-Cardo, C., Guise, T.A., and Masssague, J. (2003). A multigenic program mediating breast cancer metastasis to bone. Cancer Cell *3*, 537–549.

Ku, D.D., and Dai, J. (1997). Expression of thrombin receptors in human atherosclerotic coronary arteries leads to an exaggerated vasoconstrictory response in vitro. J. Cardiovasc. Pharmacol. *30*, 649–657.

Kuliopulos, A., Covic, L., Seeley, S.K., Sheridan, P.J., Helin, J., and Costello, C.E. (1999). Plasmin desensitization of the PAR1 thrombin receptor: kinetics, sites of truncation, and implications for thrombolytic therapy. Biochemistry *38*, 4572–4585.

Libby, P., and Aikawa, M. (2002). Stabilization of atherosclerotic plaques: new mechanisms and clincial targets. Nat. Med. *8*, 1257–1262.

Martin, C.B., Mahon, G.M., Klinger, M.B., Kay, R.J., Symons, M., Der, C.J., and Whitehead, I.P. (2001). The thrombin receptor, PAR-1, causes transformation by activation of Rho-mediated signaling pathways. Oncogene *20*, 1953–1963.

Muller, A., Homey, B., Soto, H., Ge, N., Catron, D., Buchanan, M.E., McClanahan, T., Murphy, E., Yuan, W., Wagner, S.N., et al. (2001). Involvement of chemokine receptors in breast cancer metastasis. Nature *410*, 50–56.

Murray, G.I., Duncan, M.E., O'Neil, P., McKay, J.A., Melvin, W.T., and Fothergill, J.E. (1998). Matrix metalloproteinase-1 is associated with poor prognosis in oesophageal cancer. J. Pathol. *185*, 256–261.

Nelken, N.A., Soifer, S.J., O'Keefe, J., Vu, T.-K.H., Charo, I.F., and Coughlin, S.R. (1992). Thrombin receptor expression in normal and atherosclerotic human arteries. J. Clin. Invest. *90*, 1614–1621.

Nelson, A.R., Fingleton, B., Rothenberg, M.L., and Matrisian, L.M. (2000). Matrix metalloproteinases: biological activity and clinical implications. J. Clin. Oncol. *18*, 1135–1149.

Nierodzik, M.L., Kajumo, F., and Karpatkin, S. (1992). Effect of thrombin treatment of tumor cells on adhesion of tumor cells to platelets in vitro and metstasis in vivo. Cancer Res. *52*, 3267–3272.

Nierodzik, M.L., Chen, K., Takeshita, K., Li, J.J., Huang, Y.Q., Feng, X.S., D'Andrea, M.R., Andrade-Gordon, P., and Karpatkin, S. (1998). Protease-activated receptor 1 (PAR-1) is required and rate-limiting for thrombin-enhanced experimental pulmonary metastasis. Blood *92*, 3694–3700.

Odake, S., Morita, Y., Morikawa, T., Yoshida, N., Hori, H., and Nagai, Y. (1994). Inhibition of matrix metalloproteinases by peptidyl hydroxamic acids. Biochem. Biophys. Res. Commun. *199*, 1442–1446.

Riewald, M., Kravchenko, V.V., Petrovan, R.J., O'Brien, P.J., Brass, L.F., Ulevitch, R.J., and Ruf, W. (2001). Gene induction by coagulation factor Xa is mediated by activation of protease-activated receptor 1. Blood *97*, 3109–3116.

Riewald, M., Petrovan, R.J., Donner, A., Mueller, B.M., and Ruf, W. (2002). Activation of endothelial cell protease activated receptor 1 by the protein C pathway. Science *296*, 1880–1882.

Ross, D.T., Scherf, U., Eisen, M.B., Perou, C.M., Rees, C., Spellman, P., Iyer, V., Jeffrey, S.S., Van de Rijn, M., Waltham, M., et al. (2000). Systematic variation in gene expression patterns in human cancer cell lines. Nat. Genet. *24*, 227–235.

Seeley, S., Covic, L., Jacques, S.L., Sudmeier, J., Baleja, J.D., and Kuliopulos, A. (2003). Structural basis for thrombin activation of a protease-activated receptor: Inhibition of intramolecular liganding. Chem. Biol. *10*, 1033–1041.

Sternlicht, M.D., and Werb, Z. (2001). How matrix metalloproteinases regulate cell behavior. Annu. Rev. Cell Dev. Biol. *17*, 463–516.

Tsopanoglou, N.E., and Maragoudakis, M.E. (1999). On the mechanism of thrombin-induced angiogenesis. J. Biol. Chem. *274*, 23969–23976.

van't Veer, L.J., Dai, H., van de Vijver, M.J., He, Y.D., Hart, A.A., Mao, M., Peterse, H.L., van der Kooy, K., Marton, M.J., Witteveen, A.T., et al. (2002). Gene expression profiling predicts clinical outcome of breast cancer. Nature *415*, 530–536.

Vu, T.-K.H., Hung, D.T., Wheaton, V.I., and Coughlin, S.R. (1991). Molecular cloning of a functional thrombin receptor reveals a novel proteolytic mechanism of receptor action. Cell *64*, 1057–1068.

Whitehead, I., Kirk, H., and Kay, R. (1995). Expression cloning of oncogenes by retroviral transfer of cDNA libraries. Mol. Cell. Biol. *15*, 704–710.

Yamamoto, A., Yano, S., Shiraga, M., Ogawa, H., Goto, H., Miki, T., Zhang, H., and Sone, S. (2002). A third-generation matrix metalloproteinase (MMP) inhibitor (ONO-4817) combined with docetaxel suppresses progression of lung micrometastasis of MMP-expressing tumor cells in nude mice. Int. J. Cancer *103*, 822–828.

Yin, Y.-J., Salah, Z., Maoz, M., Ram, S.C.E., Ochayon, S., Neufeld, G., Katzav, S., and Bar-Shavit, R. (2003). Oncogenic transformation induces tumor angiogenesis: a role for PAR1 activation. FASEB J. *17*, 163–174.

Youngs, S.J., Ali, S.A., Taub, D.D., and Rees, R.C. (1997). Chemokines induce migrational responses in human breast carcinoma cell lines. Int. J. Cancer *71*, 257–266.

Zain, J., Huang, Y., Feng, X.S., Nierodzik, M.L., Li, J.-J., and Karpatkin, S. (2000). Concentration-dependent dual effect of thrombin on impaired growth/apoptosis or mitogenesis in tumor cells. Blood *95*, 3133–3138.

Zucker, S., Mirza, H., Conner, C.E., Lorenz, A.F., Drews, M.H., Bahou, W.F., and Jesty, J. (1998). Vascular endothelial growth factor induces tissue factor and matrix metalloproteinase production in endothelial cells: conversion of prothrombin to thrombin results in progelatinase A activation and cell proliferation. Int. J. Cancer *75*, 780–786.

Supplemental Data

PAR1 Is a Matrix Metalloprotease-1 Receptor that Promotes Invasion and Tumorigenesis of Breast Cancer Cells

Adrienne Boire, Lidija Covic, Anika Agarwal, Suzanne Jacques, Sheida Sherifi, and Athan Kuliopulos

A

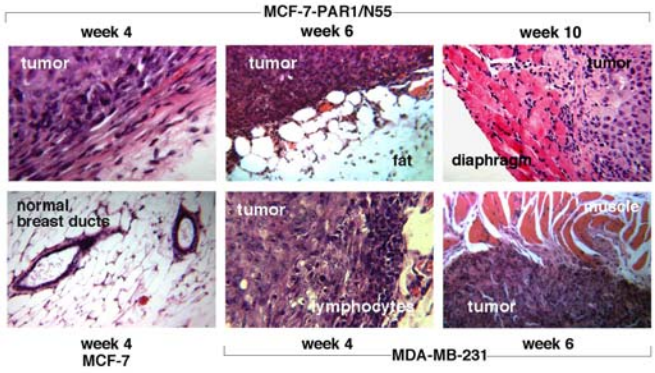

B

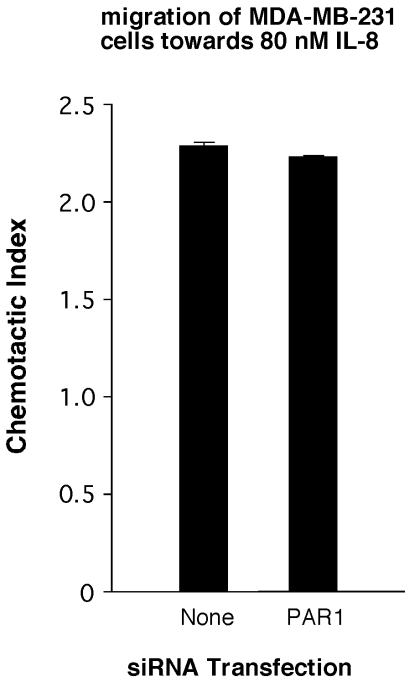

Supplemental Figure S1.

(A) Histopathology of Paraffin-Embedded Tissue Sections from PAR1-Expressing Breast Cancer Xenografts

Top row: MCF7-PAR1 clone N55 tumors were harvested from the mouse mammary fat pad (L and middle) or from the diaphragm (top R) at the indicated week postinoculation (see Figure 1). Bottom row (L to R): MCF-7-inoculated breast tissue was harvested at 4 weeks and MDA-MB-231-derived tumor was harvested at 4 and 6 weeks postinoculation, respectively.

(B) Gene Silencing of PAR with siRNA Does Not Affect Migration of MDA-MB-231 Cells Toward IL-8

siRNA treatment and migration assays were performed as described in Figure 1 except that wells were precoated with 7 μg fibronectin per 6.5 mm well, and 80 nM IL-8 agonist was placed in the lower chamber in 0.1% FBS/RPMI and migration was for 18 hr. Chemotactic index (mean ± 1 SD of duplicates) were calculated as ratio of cells migrated toward an IL-8 chemokine gradient to cells migrated in the absence of IL-8 (0.1% FBS.RPMI alone). Basal migration was approximately 750 cells migrated per filter.

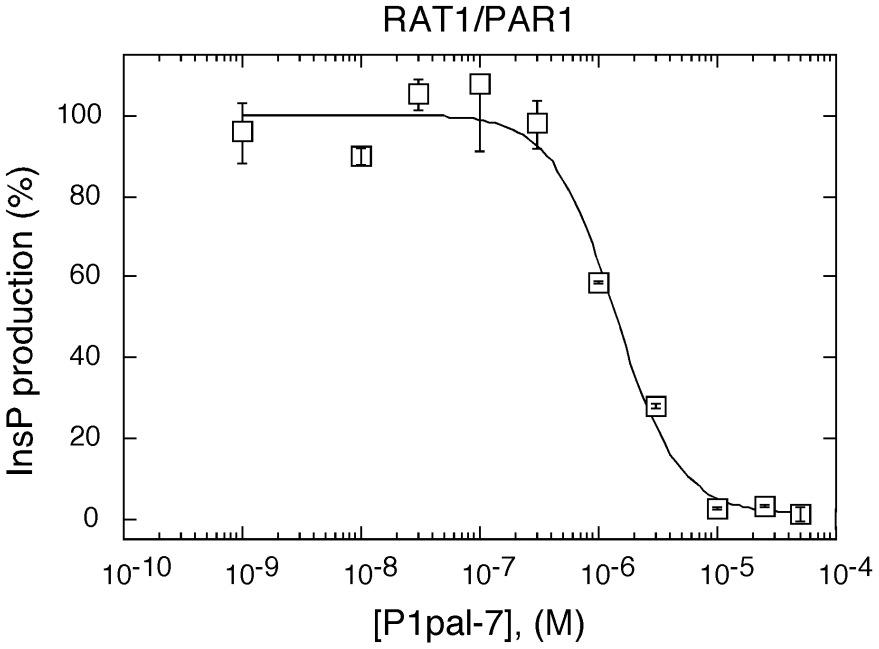

Supplemental Figure S2. The Cell-Penetrating PAR1 i3 Loop Pepducin, P1pal-7, Is a Full Antagonist of PAR1-G Protein Signaling

Stably transfected PAR1-Rat1 cells were challenged for 30 min with 0.1 nM thrombin in the presence of 1 nM to 50 μM P1pal-7 (Covic et al., 2002). PLC-β activity was determined by measuring total [^{3}H]-inositol phosphate (InsP) formation (Seeley et al., 2003). PLC-β activity was converted to percent of the full response relative to 0.1 nM thrombin (100%) and plotted as a function of P1pal-7 concentration.

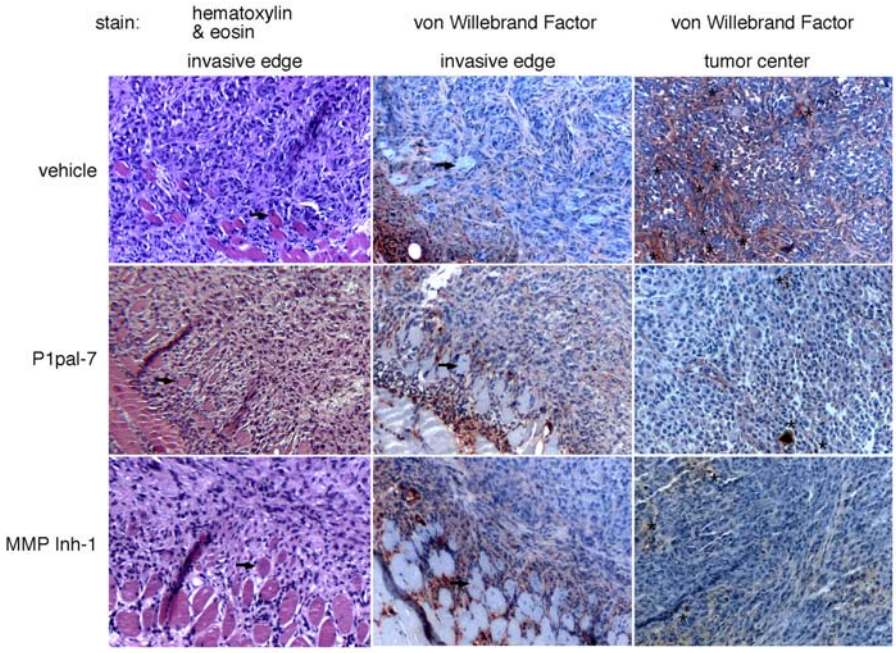

Supplemental Figure S3. Histopathology and von Willebrand Factor Staining of Paraffin-Embedded Tissue Sections From PAR1-Expressing Breast Cancer Xenografts Treated with P1pal-7 or MMP Inh-1

MCF7-PAR1/N55 xenografts and surrounding tissue were harvested from mice treated with vehicle (top row), P1pal-7 pepducin (middle row), or MMP Inh-1 (bottom row) at the conclusion of the experiment described in Figure 7C. Tumors were fixed in 10% formalin/PBS and imbedded in paraffin. Tissue sections (5 μm) were prepared and stained with hematoxylin-eosin (H&E) for histopathological analyses (L column) and with a rabbit polyclonal anti-von Willebrand Factor (vWF) (Dako) for immunohistochemistry (middle and R columns). Following blinded procedures, a pathologist examined the H&E and vWF-stained sections (n = 2–4) from each tumor (n = 4 tumors from each treatment group) and determined the morphology, invasive edge, and vascularity. To determine vascular density of the central tumor mass, five fields of the vWF-stained sections (160× magnification) from each tumor were counted. The mean (± 2 SEM) blood vessel density was 10.4 ± 2.2 for the untreated group, 2.6 ± 1.0 ($p = 0.002$) for the P1pal-7-treated group, and 3.6 ± 1.5 ($p = 0.006$) for the MMP Inh-1-treated group. The Plpal-7- and MMP Inh-1-treated groups did not have significantly different ($p = 0.30$) mean blood vessel density. Arrows denote skeletal muscle; * denote vWF staining of endothelial cells.

Supplemental References

Covic, L., Gresser, A.L., Talavera, J., Swift, S., and Kuliopulos, A. (2002). Activation and inhibition of G protein-coupled receptors by cell-penetrating membrane-tethered peptides. Proc. Natl. Acad. Sci. USA *99*, 643–648.

Seeley, S., Covic, L., Jacques, S.L., Sudmeier, J., Baleja, J.D., and Kuliopulos, A. (2003). Structural basis for thrombin activation of a protease-activated receptor: Inhibition of intramolecular liganding. Chem. Biol. *10*, 1033–1041.